Journal Pre-proof

Eco-Friendly Selective Laser Sintered (SLS) 3D Printing of Tablets Using Starch 1500® as a Standalone Green Excipient

Sujith Raj Bashetty , Yu Zhang , Navya Nalajala , Thirupathi Reddy Anekalla , Lakshmi Priyanka Gudipati , Nagarjuna Narala , Rohith Alluri , Mohammed Maniruzzaman

PII: S2666-8939(26)00067-8
DOI: https://doi.org/10.1016/j.carpta.2026.101153
Reference: CARPTA 101153

To appear in: *Carbohydrate Polymer Technologies and Applications*

Received date: 5 March 2026
Revised date: 28 April 2026
Accepted date: 11 May 2026

Please cite this article as: Sujith Raj Bashetty , Yu Zhang , Navya Nalajala , Thirupathi Reddy Anekalla , Lakshmi Priyanka Gudipati , Nagarjuna Narala , Rohith Alluri , Mohammed Maniruzzaman , Eco-Friendly Selective Laser Sintered (SLS) 3D Printing of Tablets Using Starch 1500® as a Standalone Green Excipient, *Carbohydrate Polymer Technologies and Applications* (2026), doi: https://doi.org/10.1016/j.carpta.2026.101153

This is a PDF file of an article that has undergone enhancements after acceptance, such as the addition of a cover page and metadata, and formatting for readability, but it is not yet the definitive version of record. This version will undergo additional copyediting, typesetting and review before it is published in its final form, but we are providing this version to give early visibility of the article. Please note that, during the production process, errors may be discovered which could affect the content, and all legal disclaimers that apply to the journal pertain.

© 2026 Published by Elsevier Ltd.
This is an open access article under the CC BY-NC-ND license (http://creativecommons.org/licenses/by-nc-nd/4.0/)

Journal Pre-proof

Eco-Friendly Selective Laser Sintered (SLS) 3D Printing of Tablets Using Starch 1500® as a Standalone Green Excipient

Sujith Raj Bashetty, Yu Zhang*, Navya Nalajala, Thirupathi Reddy Anekalla, Lakshmi Priyanka Gudipati, Nagarjuna Narala, Rohith Alluri, Mohammed Maniruzzaman*

Pharmaceutical Engineering and 3D Printing (PharmE3D) Lab, Department of Pharmaceutics and Drug Delivery, School of Pharmacy, The University of Mississippi, University, MS 38677, United States

*Corresponding author: mmaniruz@olemiss.edu; Co-Corresponding author: yuzhang@olemiss.edu

Keywords

Carbohydrate Polymers; Personalized Medication; Selective Laser Sintering; Laser Speed; Amorphous Solid Dispersion; Green Excipient; Oral Solid Dosage Forms.

Abstract

Carbohydrate-based polymers are increasingly recognized as sustainable materials for additive manufacturing. For the first time, Starch 1500®, a partially pregelatinized maize starch, was used as the sole excipient in selective laser sintering (SLS) 3D printing of tablets. While previous studies relied on solubilizers or complex excipient blends, our approach shows that robust indomethacin (IND) tablets can be fabricated using only Starch 1500® or in combination with Kollidon® VA64, without the addition of surfactants or plasticizers. Optimized laser scanning (200-300 mm/s) created tablets that were mechanically strong and free of defects. The IND was completely amorphized, except for a minimal trace of crystallinity in one formulation. Dissolution studies conducted under a pH-shift protocol exhibited significantly improved release; starch-only tablets attained over 80% release within 45 minutes at pH 6.8, in contrast to approximately 23% for crystalline drug, whereas VA64 maintained supersaturation. Powder reusability exhibited no degradation, hence promoting sustainability. For quality control, an HPLC method that indicates stability was developed and validated (ICH Q2(R2)). This starch-enabled SLS platform highlights an excipient-minimum additive manufacturing approach and a sustainable, patient-tailored dose form. Thus, our research opens new possibilities for advancing eco-conscious pharmaceutical manufacturing through SLS 3D printing, especially in developing formulations that align with sustainability goals in the industry.

Journal Pre-proof

1. Introduction

Additive manufacturing is gaining traction in pharmaceutical development as a flexible, solvent-free route to produce patient-centric oral dosage forms with tunable geometry, porosity, and release behavior (Gueche et al., 2021; Zhang et al., 2023). The first attempt at using 3D printing (3DP) technology in pharmaceuticals dates back to 1996 (Wu et al., 1996), and the first selective laser sintering (SLS) printed pharmaceutical dosages were applied in 2017 (Fina et al., 2017a). SLS processes a bed of pharmaceutical powders using a laser to sinter particles with special patterns layer by layer. The technique allows quick on-demand production, minimal tooling, and efficient use of material (Kruth et al., 2003, 2005). While SLS has been applied to several active pharmaceutical ingredients, its broader adoption has been limited by two practical constraints in pharmaceutics. First, there is a small set of excipients that both print reliably under SLS thermal conditions and support immediate or modified release without the need for additional formulation aids such as plasticizers or surfactants (Kumar, 2003; Murkute et al., 2022; Trenfield et al., 2018). Second, there is a need for release assays that are demonstrably stability-indicating and validated to current regulatory expectations, since laser exposure, elevated build temperatures, and sintering agents can introduce matrix effects and unique degradant profiles that differ from conventionally manufactured tablets (Fina et al., 2018; A. G. Tabriz et al., 2023).

Carbohydrate-based polymers offer a sustainable pathway to address the excipient gap. Starch 1500®, a partially pregelatinized maize starch, is a multifunctional excipient with binding, disintegrant, and flow-enhancing properties (Di et al., 2022; Su et al., 2021). Its dual nature, with amorphous regions that soften near processing temperatures and residual crystallinity that preserves particle integrity during spreading, suggests it may enable direct SLS printing without additional binders. In parallel, hydrophilic vinylpyrrolidone-vinyl acetate copolymers such as Kollidon® VA64 are known to stabilize amorphous solid dispersions and maintain supersaturation during dissolution. A rational combination of Starch 1500® with Kollidon® VA64, therefore, has the potential to pair diffusion-controlled hydration and erosion of the starch matrix with polymer-enabled supersaturation control, yielding robust printability and enhanced release from simple, surfactant-free formulations (Barakh Ali et al., 2019).

Indomethacin (IND) is a poorly water-soluble, weakly acidic model drug that has been widely used to probe amorphization and dissolution enhancement in thermally driven processes. For SLS, the key scientific questions are whether a starch-based powder bed can be sintered at process temperatures that preserve drug integrity, whether the rapid localized heating can induce in situ amorphization without recrystallization during cooling and storage, and how formulation composition and laser parameters govern mechanical properties and *in vitro* performance (Thakkar, Jara, et al., 2021; Thakkar, Zhang, et al., 2021; Yang et al., 2021). These questions are coupled to an analytical need. Quality control for SLS printlets requires a release

method that is specific for IND in the presence of excipients and laser absorbers, that resolves likely degradants generated under acidic or basic stress, oxidation, heat, and light, and that is validated per ICH Q2(R2) for specificity, linearity, accuracy, precision, range, sensitivity, robustness, and solution stability (Nováková et al., 2005).

In this research, we addressed the formulation gap and developed and validated a simple, robust analytical method. We investigate Starch 1500® as a primary excipient for SLS of IND tablets, either as the sole matrix former or in binary blends with Kollidon® VA64, using a pharmaceutical pearlescent pigment as the laser energy absorber (the sintering agent). The powder flow and bed-forming behavior were evaluated. Also, we define a practical SLS process window by systematically varying laser scan speed while maintaining build and surface temperatures appropriate for excipient softening without API degradation. Solid-state and structural characterization by differential scanning calorimetry, Fourier transform infrared spectroscopy, powder X-ray diffraction, and proton nuclear magnetic resonance are used to confirm amorphization and probe drug–excipient interactions. Tablet geometry, mass uniformity, and mechanical integrity are quantified to link process conditions to print quality. *In vitro* dissolution is measured under a physiologically relevant pH-shift protocol to capture gastric exposure followed by intestinal conditions, allowing us to assess whether amorphization, matrix hydration, and polymer-mediated supersaturation translate to meaningful release gains relative to crystalline IND.

Because powder reuse and thermal exposure are intrinsic to powder-bed processes, we further examine chemical stability across repeated printing cycles using mass spectrometry to monitor assay and potential degradants. To enable reliable quality control, we develop a rapid reverse-phase HPLC method for IND quantitation in SLS printlets and validate it as stability-indicating to ICH Q2(R2). The method's specificity is demonstrated by baseline resolution of IND from representative degradants under forced degradation, and its performance is established across linearity, accuracy, precision, limit of detection and quantitation, robustness to small method changes, and solution-state stability over relevant storage conditions.

While several carbohydrate excipients, such as pectin, alginate, and dextran, are useful for drug delivery, they usually work well as hydrogels for extrusion/inkjet routes and frequently require blending or modification to provide the powder flow and thermal softening needed for powder-bed laser sintering methods (Aghajani et al., 2025; Chang et al., 2023; Sabbatini et al., 2021; A. Tabriz et al., 2025; A. G. Tabriz et al., 2023; Wei et al., 2023; Zarandona et al., 2021). Only a small subset of polymers consistently sinters, and blue-diode systems often need absorbers to couple energy into the bed, as highlighted by recent SLS-focused reviews and polymer-suitability studies (Balasankar et al., 2023; A. Tabriz et al., 2025). These findings highlight the processing limitations for polysaccharides that lack intrinsic softenability. Starch 1500®, on the other hand, is a

pharmaceutical/food-grade, partially pregelatinized maize starch that is compendial and has binder–disintegrant duality, improved flow/compatibility compared to native starch, and moisture-scavenging (low water activity) that can stabilize sensitive APIs (Aghajani et al., 2025; Wei et al., 2023; Zarandona et al., 2021). These characteristics are directly related to SLS powder spreading, interparticle fusion, and downstream performance (PA Cuthbert & Co, 2023). Its proven regulatory acceptance and scalability give it an advantage over niche biopolymers that require modification or blending for printability.

Based on the excipient gap in SLS 3DP, we propose that the partially pregelatinized structure of Starch 1500® supports direct powder fusion and promotes in situ amorphization of indomethacin without plasticizers or surfactants (Colorcon, 2019). This study further hypothesized that binary blends with Kollidon® VA64 would combine rapid hydration/disintegration from starch with polymer-mediated supersaturation control to improve release across gastrointestinal pH conditions, enabling simplified, sustainable, patient-specific manufacturing supported by a validated stability-indicating analytical workflow. The goal is to make SLS formulation design easier, reduce the number of excipients needed, and create a viable path to sustainable, patient-specific production by combining this formulation technique with a validated, stability-indicating analytical technology.

2. Materials and Methods

2.1 Materials

Table 1 Physicochemical properties of active pharmaceutical ingredient (API) and polymers (Anastasiades et al., 2002; Angupale et al., 2020; Bühler, 2008; Corrigan et al., 1985; Davis Jr et al., 2020; Eraga et al., 2024; Hong & Liu, 2023; Imaizumi et al., 1980; Maddineni et al., 2015; Musumeci et al., 2025; Pratik et al., 2019; Simpson, 2000)

Journal Pre-proof

Compound	Chemical Structure	Molecular Weight	Melting/glass transition temperature (T_g /T_m) ℃	Properties
Indomethacin	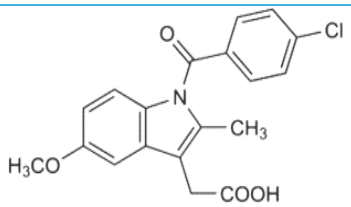	357.79 (g/mol)	T_m: 160-162	Non-steroidal anti-inflammatory drug (NSAID); poorly soluble
Starch® 1500	Amylose (73%) 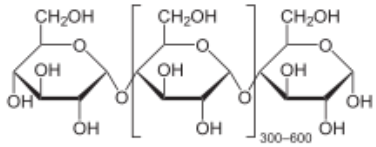 Amylopectin (27%) 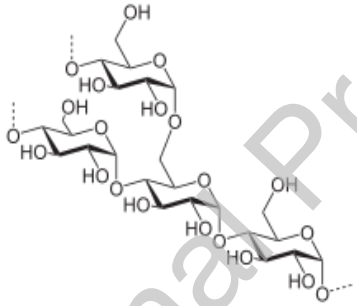	90,000-300,000 g/mol	T_m: 256-268	Partially pregelatinized maize starch; good binding properties; acts as a disintegrant, filler, flow aid, and lubricant. PSD: 10-70 µm
Kollidon® VA64	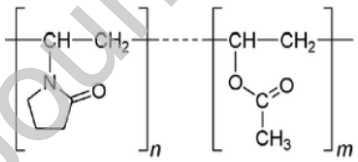	45,000 - 70,000 Da	Tg: 106	Copolymer of vinylpyrrolidone and vinyl acetate; binder
Candurin® Gold Sheen	Natural mica coated with titanium dioxide (TiO_2) and iron oxide (Fe_2O_3), Gold Pearlescent pigment	N/A	N/A	PSD: 5-25 µm, Acts as a sintering agent

Indomethacin was purchased from Tokyo Chemical Industries (Tokyo, Japan) and was used as a model drug. Starch 1500® (Partially Pregelatinized Maize Starch) was gifted by Colorcon (Indianapolis, USA). Kollidon® VA64 is a vinylpyrrolidone-vinyl acetate copolymer with an average molecular weight of 65,000 g/mol, donated by BASF Corporation (Tarrytown, NY, USA). Candurin® Gold Sheen was gifted to the Lab from EMD Performance Materials Corp. (Philadelphia,

PA, USA). Monohydrate and dihydrate sodium phosphate salts were purchased from Fisher Scientific™ (Pittsburgh, PA, USA). HPLC-grade acetonitrile and methanol were purchased from Fisher Scientific™ (Pittsburgh, PA, USA). All the other chemicals and reagents were ACS grade or higher and their properties listed in Table 1.

2.2 Preparation of Powder Blends and Formulation Design

Table 2 Composition of indomethacin–starch–polymer powder blends used for SLS printing.

Formulation code (% w/w)	INDOMETHACIN (IND)	STARCH® 1500	Kollidon® VA64	CANDURIN® Gold sheen
F1	20	77	0	3
F2	20	67	10	3
F3	20	57	20	3
F4	20	47	30	3
F5	20	27	50	3
F6	20	0	77	3

Pharmaceutical powder blends were mixed by geometric dilution of the active pharmaceutical ingredient (API), sieved through a 150 µm pore diameter (100 mesh) and stored in sealed container until printing. The formulation components included Starch 1500® and Kollidon® VA64 as excipients, along with Candurin® Gold Sheen as a sintering agent. Based on prior research findings (Thakkar, Zhang, et al., 2021) Indomethacin was fixed at 20% w/w, and Candurin® Gold Sheen at 3% (Zhang et al., 2023) in all blends. The compositions detailed in Table 2 were systematically designed to assess the effect of varying Starch 1500® on sintering behavior, printability, and dissolution.

2.3 Selective Laser Sintering 3D printing process

Oval Printlets (12 mm diameter × 3 mm height) were designed using 3D Builder software (version 18.0.1931.0, Microsoft Corporation) and exported as standard tessellation language (.stl) files. The total tablet weight was designed to achieve 300 mg of drug per dosage form. These files were sliced in Sintratec Central (v 1.2.9, Sintratec), and the oral dosage forms were fabricated using a desktop SLS 3D printer (Sintratec Kit, AG, Brugg, Switzerland), equipped with a 2.3 W blue diode laser (λ=445 nm) with a reservoir platform and building platform of 150 mm × 150 mm × 150 mm. To enhance laser energy absorption and enable effective sintering, Candurin® Gold Sheen, a pharmaceutical pigment, was incorporated as a laser absorbent (21 CFR 73.3128, 2024; fda.gov/industry/color-additives, 2019; Mohamed, 2020). All F1 to F6 formulations were printed

under similar SLS conditions except laser speed, which was tested at 200, 250, and 300 mm/s. Surface and chamber temperatures were 80 and 105 °C. A hatching space of 25 with a 120 µm hatching offset, and with a 200 µm perimeter offset, each tablet was printed with a single perimeter. The layer height was 100 µm. Printing temperature and laser scan speed were tuned to the glass-transition temperature of each polymer to achieve complete particle fusion and produce mechanically robust dosage forms.

2.4 Powder blend characterization

2.4.1 Blend Uniformity

Blend uniformity (n=3) was performed to ensure homogeneous distribution of API within the prepared blends. Ten aliquots (100 mg each) were randomly sampled from different locations of the powder bed (Léonard et al., 2008; Narala et al., 2023), dissolved in methanol, and sonicated for 20 min. The extract was diluted 100 times, filtered through a 0.45 µm membrane, and analyzed by HPLC-UV. Indomethacin content was quantified, and the mean and relative standard deviation (RSD) were recorded.

2.4.2 Flowability Test (Bulk and Tapped Density)

The Compressibility Index (Carr's Index, I), Hausner's Ratio, was investigated by measuring the tapped and bulk densities of the powder (Nyavanandi et al., 2021; Suwanprateeb et al., 2010). Bulk density was determined using a 100 mL graduated cylinder, and tapped density was measured after 1250 taps using TD1- one compact tapped density tester (SOTAX, USA) as described in the United States Pharmacopeia (European Medicines Agency (EMA)(Ph. Eur. 2.9.34), 2013; USP (616), 2015) in one compact unit. Comparison of the bulk and tapped densities with the Compressibility Index and Hausner Ratio indicates the ability of the powder to flow and settle. The Carr's Index of the blend was calculated using the following equation:

$$I\ (\%) = 1 - (V - V_0) \times 100,$$

where CI is the Carr's index, and V_O and V are the initial and final (tapped) powder volumes, respectively, of the blend in the measuring cylinder.

2.4.3 Angle of Repose

The angle of repose was determined by pouring a measured amount of powder onto a horizontal surface to form a conical pile using PF 1 flowability testing (SOTAX, USA). The height and base

diameter of the resulting cone were measured to calculate the angle of repose, which indicates the powder's flow characteristics and its tendency to pile up. Measurements (n=3) were performed to ensure the reliability and reproducibility of the results (Nyavanandi et al., 2021). The angle of repose was calculated using the following equation:

$$\text{Angle of Repose } (\theta) = tan - 1 \times height\ of\ cone, mm/50\ mm$$

2.4.4 Mass spectrometry

Chemical profiling and stability assessment of the printed powders were performed using UPLC–MS. The Waters Acquity UPLC system (Waters Corp., Milford, USA) with a BEH C18 column (100 × 2.1 mm, 1.7 µm) was used to achieve chromatographic separation. The data were processed with MassLynx v4.2 workstation (Hess et al., 2001). All other details about instrument wash solutions and additional MS/MS parameters are provided in the Supplementary Method S1.

2.5 Thermal and chemical analysis

2.5.1 Differential Scanning Calorimetry (DSC)

The thermal analysis for Indomethacin (IND), excipients, physical mixtures, and the printed tablets was evaluated by the Discovery DSC 25 instrument (TA Instruments, located in New Castle, DE, USA). Samples weighing 5.1 to 5.7 mg were precisely measured and sealed into standard aluminum DSC pans. An empty pan served as the reference. The samples were heated at 10°C per minute, over a temperature range of 25°C to 250°C. Data analysis was performed using TRIOS software (TA Instruments), and the results were presented as temperature (°C) versus reverse heat flow (mW) (Bhatkande et al., 2024). This method ensured accurate thermal characterization of the materials and formulations.

2.5.2 Fourier transform infrared spectroscopy (FTIR)

To evaluate the drug-excipient compatibilities, FTIR spectra of the API, excipients, physical mixtures, and the crushed powder of printed tablets were tested using a Cary-360 FTIR spectrometer (Agilent Technologies, Santa Clara, CA, USA), and sampling was performed using a MIRacle Attenuated Total Reflection (Pike Technologies MIRacle ATR, Madison, WI, USA) (Thakkar, Zhang, et al., 2021). ~10-15 mg of samples was analyzed for transmittance (%) versus

wavenumber from 650-4000 cm^{-1}, at a resolution of 4 cm^{-1} and 32 scans per run. Absorbance and Transmittance modes were used. MINILAB OC series software (Version 9.0 ThermoFisher Scientific, Waltham, MA, USA) was used to capture and analyze the spectra (Pillai A, 2023).

2.5.3 Powder X-ray diffraction (pXRD)

Powder X-Ray Diffraction (pXRD) to evaluate crystallinity was conducted on an AXRD benchtop from Proto Manufacturing. The instrument is equipped with an X-ray copper radiation source utilizing a current of 15 mA and a voltage set at 40 kV. Using aluminum sample holders, a two-theta range of 5 to 80° was scanned at 1.0°/min using a step size of 0.01° while samples were rotated. Data was analyzed using MDI JADE 9 software (Materials Data Inc., Livermore, CA). To ensure accuracy and reliability, samples were performed in triplicate(Maniruzzaman et al., 2017).

2.5.4 ^{1}H Nuclear Magnetic Resonance (NMR) Spectroscopy

The structural identity of the pure indomethacin and its formulations was confirmed using ^{1}H nuclear magnetic resonance (^{1}H-NMR) spectroscopy. For NMR analysis (Pham et al., 2010). 10 mg of the sample was dissolved in 600 µL of deuterated DMSO-d_6 and analyzed using a Bruker Advance DRX 400 MHz Avance IIIHD spectrometer at 298 K. The acquired spectral data was processed and analyzed using the MestReNova 14.3.1 software.

2.6 Printlets Characterization

2.6.1 Printlet Morphology and Microscopy

The diameter and height of the printed tablets (n=10) were determined using a digital caliper (DigiMax®, Dublin, Ireland), and tablet weight was measured with a Fisher Brand analytical balance (Fisher Scientific, Leicestershire, UK), with results reported as mean ± standard deviation. Furthermore, the images of the tablets (n = 3) were captured using a Dino-Lite Edge AM7391MZTL optical microscope (AnMo Electronics Corporation, New Taipei, Taiwan), and a scale bar was integrated for visual measurement.

2.6.2 Scanning Electron Microscopy

The surface morphology of the optimized IND printed tablets formulation was examined using a JSM-7200FLV Scanning Electron Microscope (SEM) (JEOL, Peabody, MA, USA), operated at an

accelerating voltage of 3 kV and 8 kV. Printlets were mounted onto SEM stubs using double adhesive carbon tape. To ensure conductivity during imaging, the samples were sputter-coated under an argon atmosphere using a Denton Desk V TSC Sputter Coater (Denton Vacuum, Moorestown, NJ, USA). The coating materials used included a 60:40 gold-palladium alloy for surface imaging. The imaging was conducted at magnifications up to 50x, 100x and 250x enabling a detailed examination of the surface structure and pore size of the SLS 3D printed tablets. The selected coating techniques and imaging parameters ensured high-resolution visualization of the surface characteristics, providing insights into the morphology of the printlets.

Tablet density was determined from tablet weight and geometric volume of the printed tablets. The volume of the oval tablets were estimated using elliptical cylinder approximation below

$$V = \pi/4 \times L \times W \times T,$$

where L, W and T are measured length, width and thickness respectively depicted in supplementary information *TableS2* .The apparent density (ρ_{tablet}) was then calculated as the ratio of mass to its calculated volume of tablets.

Porosity (%) was calculated from the below equation

$$\text{Porosity} = (1 - \rho_{tablet}/\rho_{true}) \times 100$$

Where the ρ_{tablet} is the estimated tablet density and ρ_{true} is the true is the real density of the formulation, where experimentally determined real density was not available, a theoretical density value was assumed based on weighted contribution of formulation components.

2.6.3 Determination of mechanical properties

Tablet hardness was evaluated using a digital hardness tester (VK 200 Tablet Hardness Tester). Oval-shaped tablets (n = 10) were visually inspected for any physical defects before testing. Each tablet was positioned with its longer side (major axis) lying flat and parallel to the testing surface. The force required to break each tablet (measured in kilopascals, KPa) was recorded. The mean and SD were recorded.

2.7 HPLC Analytical Method Development and Validation

A stability-indicating reverse-phase high-performance liquid chromatography (RP-HPLC) method was developed and validated to quantify Indomethacin in SLS tablets. In the present study, validation of the developed HPLC method was conducted in accordance with the ICH Q2(R2) guideline (EMA|ICH Q2(R2), 1994). The validation process encompassed a thorough assessment of key parameters, including specificity, linearity, range, accuracy, precision, solution stability, sensitivity (expressed as LOD and LOQ), and robustness. Detailed experimental procedures, acceptance criteria, and results for all validation parameters and forced degradation studies are provided in Supplementary Method S2.

2.8 Drug Assay

The drug content of the printed tablets (n=3) was determined in accordance with the USP monograph USP43-NF38 for Indomethacin (USPNF Monograph, 2025). Each tablet was accurately weighed (equivalent to 60 mg API), dissolved in methanol (15mL) in a scintillation vial, and sonicated for 20 minutes. The solution was diluted 100-fold and filtered through a 0.45 µm membrane and analyzed for drug content.

2.9 *In vitro* dissolution studies

The In-vitro release testing of the 3D-printed tablets of all the formulations was compared to that of pure crystalline Indomethacin (IND). For this dissolution study, Transit media was used to mimic physiological conditions. Initially, the samples (n=3) were introduced in 750 mL of 0.1 N hydrochloric acid (HCl) buffer (pH 1.2, Acidic Buffer) for 2 hours. To achieve the pH shift, 250 mL of concentrated phosphate buffer solution (PBS, 0.1 M) was added to each vessel and made up to a final volume of 1000 mL, resulting in a medium from pH 1.2 to pH 6.8. Care was taken to prepare the phosphate buffer such that, upon dilution, the final volume maintained the desired pH 6.8 condition. The dissolution of the samples was tested at the final pH of 6.8 for an additional 6 h. The dissolution testing was conducted using a USP type I apparatus (Basket method) with a dissolution Autosampler (Agilent Technologies, Santa Clara, California, USA) at 37.5°C, with the rotation set at 75 RPM throughout the study. At predetermined intervals, 1.5 mL samples were taken from the dissolution media using 0.2 µm polyether sulfone filters through an autosampler (Vankel VK 8000, Agilent Technologies, Santa Clara, California, USA). To ensure consistent volume, an equal amount of fresh buffer was added back to the vessel after each sample was withdrawn.

Journal Pre-proof

The previously established analytical method was used to quantify the active pharmaceutical ingredient (API) in the collected sample.

3 Results

3.1 Selective Laser Sintering 3D Printing

In this study, a systematic evaluation of formulation compositions and SLS 3D printing process parameters were conducted to investigate the printability of Starch 1500® and its impact on the quality attributes of Indomethacin (IND)-loaded tablets. Tablets were fabricated under optimized SLS conditions, while systematically varying laser speeds to identify optimal sintering conditions and minimize the processing defects. Laser speeds between 50 and 190 mm/s consistently resulted in over-sintering and tablet charring, while speeds above 300 mm/s produced under-sintered, mechanically weak tablets. Thus, 200, 250, and 300 mm/s were selected for further evaluation.

All formulations incorporating Starch 1500®, either alone or in combination with Kollidon® VA64, successfully yielded high-quality tablets with complete amorphous conversion of Indomethacin, except F1 300 mm/s, which showed minimal crystallinity, as confirmed by solid-state characterization techniques. The success rate of the printing was consistent across all the formulations, with 100% printability achieved within the optimized laser speeds from 200-300mm/s. However, qualitative differences in mechanical integrity were observed, where starch rich formulations showed little brittleness over polymer rich tablets. This methodical approach allowed for a detailed examination of how these variables influenced key tablet attributes, including mechanical strength, dissolution rate, surface morphology, and crystalline drug to Amorphous form. By meticulously optimizing these parameters, a reliable printing process was established, resulting in consistent tablet production without failures or defects, and each time successfully produced 25 tablets, which were carefully removed from the building chamber. The primary goal was to determine an optimal laser speed that would produce tablets with the right balance of brittleness and hardness, avoiding defective tablets, which could impede solubility and dissolution rate.

Morphological evaluation using digital microscopy, as illustrated in Figure 1, confirmed the consistent surface texture and well-defined geometry of the printed tablets. Also, printlets that showed defective printing during process optimization are illustrated in Figure S5.1. Dimensional analysis showed close agreement with the CAD specifications, with minimal standard deviation

Journal Pre-proof

and negligible inter-batch variability depicted in Table S4.1 in supplementary information, further supporting the reproducibility of the optimized printing process.

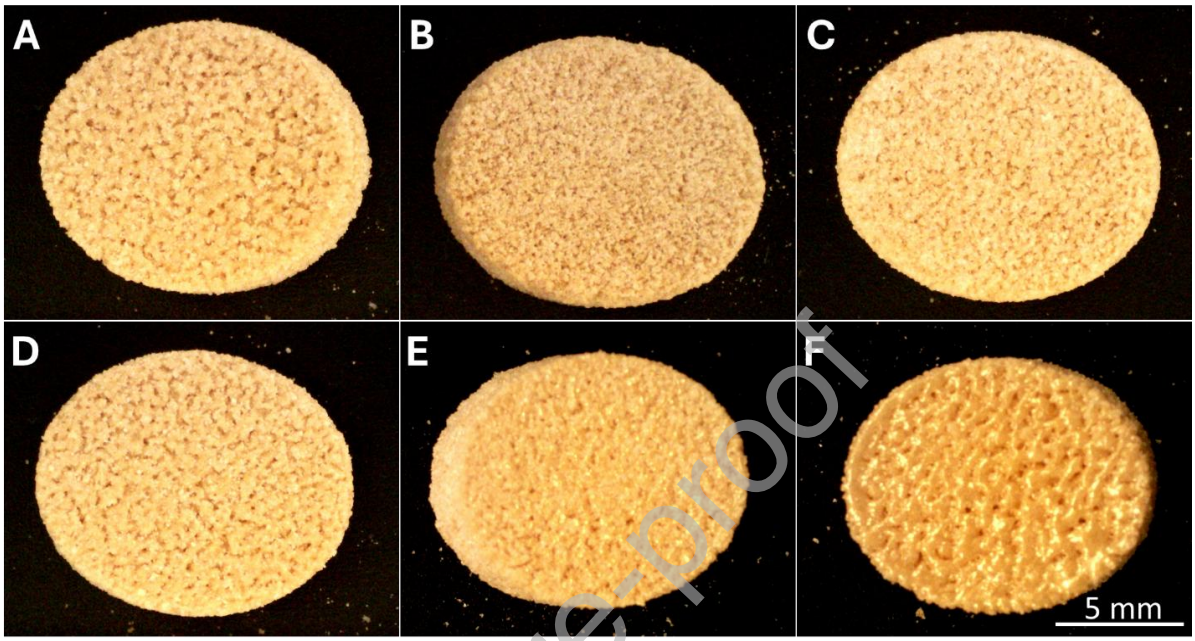

Figure 1 Images captured using Dino-Lite microscopy at optimized laser scanning conditions of A) F1 formulation, B) F2 formulation, C) F3 formulation, D) F4 formulation, E) F5 formulation, F) F6 formulation

The target weight for these tablets was set at 300 mg, and according to USP guidelines, a weight variation of up to 7.5% is permissible for tablets of this size. This means a deviation of above or below 22.5 mg from the target weight would be acceptable. However, the actual weight deviation observed in the produced tablets was minimal, falling well within this allowable range.

Moreover, the blend uniformity results indicated that the Indomethacin content in the powder mixture was within the acceptable range, demonstrating adequate homogeneity across all formulations. The average drug content value (%) in all the powder blends is listed in Table S4.2. These findings show that the mixing process was effective in achieving uniform drug dispersion, which is critical for consistent dosing and reliable performance in 3D printed dosage forms.

SEM analysis showed significant changes in the surface morphology and internal microstructure of SLS 3D Printlets (F1-F6), mainly controlled by the relative amounts of Starch 1500® and Kollidon®VA64. For the formulations with increased Starch 1500® concentration (F1-F3), more porous and heterogeneous structures were observed, characterized by irregular particle fusion, visible interparticle gaps and rough surface topology. These patterns imply incomplete coalescence of the starch particles to form an open matrix structure.

On the contrary, the formulations with increasing amount of Kollidon® VA64 presented smoother, denser and more continuous surfaces with less evident porosity and F6 has seen no porosity. An increased interparticle fusion was seen in the polymer-rich systems which resulted in a more cohesive matrix, probably due to the thermoplastic behavior of Kollidon® VA64 during the sintering process. Additionally, SEM pictures demonstrated in the Figure 2 that porosity extended throughout the tablet matrix and was not confined to the surface, indicating that the formulation composition plays a crucial role in shaping the internal microstructure of SLS printed tablets.

Tablet densities ranged from **0.800 to 1.016 g/cm³**, with porosity between **~21.8% and 38.5%**. Starch-rich formulations (F1-F3) showed lower densities (**0.832–0.895 g/cm³**) and higher porosity (**~31-36%**), while polymer-rich formulations (F4-F6) exhibited higher densities (**0.898-1.016 g/cm³**) and lower porosity (**~22-31%**). The Density increased **F1 to F6** with a corresponding decrease in porosity. Formulation composition and Laser speed both influenced these values. Higher density also corresponded to increased hardness, as observed in F6 (LS 200) (**0.938 g/cm³**, **23.09 kp**) compared to F1 (LS 300) (**0.880 g/cm³**, **1.06 kp**). Overall, density and porosity varied significantly across formulations and processing conditions, confirming their dependence on composition and laser speed.

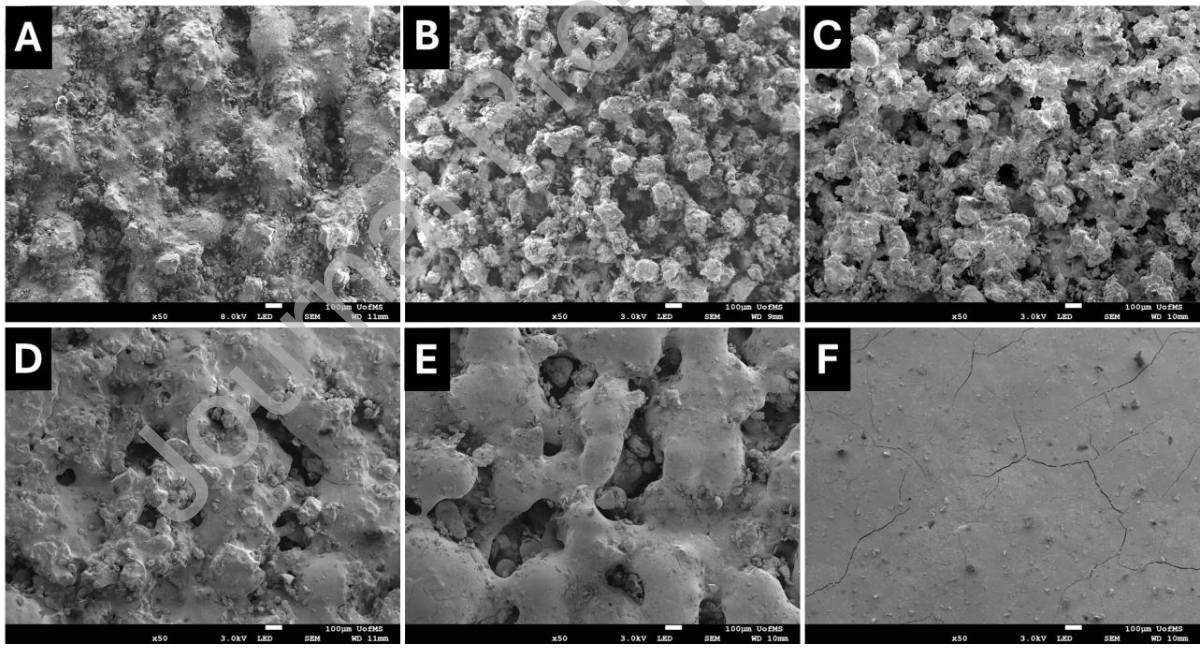

Figure 2 SEM Images showing surface and cross-sectional morphology across formulations with optimized laser scanning conditions of A) F1 formulation, B) F2 formulation, C) F3 formulation, D) F4 formulation, E) F5 formulation, F) F6 formulation

3.2 Powder flow characterization

The flowability of the powder blends for all formulations was assessed through a series of bulk property tests, including powder flow, angle of repose, tap density, bulk density, Hausner's ratio, and compressibility index according to USP Powder flow <1174> (Suwanprateeb et al., 2010; USP〈1174〉, 2024). The results for each formulation are shown in Table 3**.** The angles of repose varied slightly among formulations, but all showed substantial particle flow.

Table 3 Flow properties of powder blends prior to SLS printing.

Formulation	Bulk Density (g/cm^3)	Tap Density (g/cm^3)	Hausner's ratio	Compressibility Index (%)	The angle of Repose (°)	Classification
F1	0.61	0.83	1.30	24.90	40.8	Passable
F2	0.59	0.82	1.27	24.56	42.0	Passable
F3	0.54	0.79	1.28	23.94	41.9	Passable
F4	0.48	0.71	1.26	22.86	40.6	Passable
F5	0.44	0.68	1.54	35.06	41.3	Very poor
F6	0.39	0.56	1.42	31.08	46.2	Poor

The flowability decreased significantly with the increase of polymer content where the compressibility index increased from 22.86% (F4) to 35.06% (F5) quantitatively. Similarly, the Hausner ratio increased from 1.26 to 1.54, showing poor packing efficiency. These findings point to a definite inverse link between starch concentration and powder flow performance. Formulations F5 and F6 exhibited poor flow (CI > 30 %) which caused irregular layer spreading and localized voids during sintering, confirming that starch content ≥ 50 % is essential for uniform bed formation. Powder blends containing higher proportions of Starch 1500® (F1 to F4) displayed passable flow. In contrast, formulations dominated by Kollidon® VA64 showed a poor to very poor flow, consistent with a higher compressibility index and a higher angle of repose (>45°). Despite this, all blends could still be processed in the SLS printer, suggesting that starch improves powder spreading and compensates for the poor flow of VA64 alone (Table 3).

Journal Pre-proof

3.3 Mass spectrometry

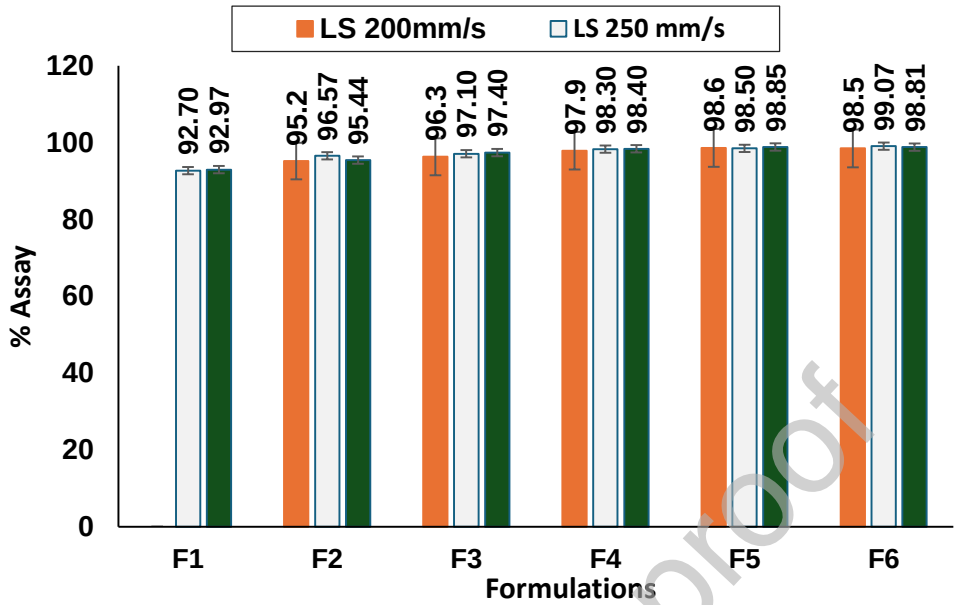

Figure 3 Indomethacin assay (%) determined by UPLC–MS after ten successive SLS powder reuse cycles at laser speeds of 200, 250, and 300 mm s^{-1}, demonstrating chemical stability during repeated processing

To assess the chemical stability and reusability of powder blends during repeated SLS 3D printing cycles, mass spectrometric analysis was performed on all formulations subjected to ten successive printing cycles. The purpose was to determine whether prolonged exposure to elevated surface and chamber temperatures, along with repeated laser irradiation at varying speeds, resulted in drug degradation or compositional changes.

In Figure 3, Formulations maintained consistent drug content across laser speeds of 200, 250, and 300 mm/s. Formulations F5 and F6 exhibited minimal assay variation, ranging between 98.48 and 99.07%, while Formulations F2, F3, and F4 demonstrated similarly acceptable ranges (95.18 and 98.40%). Although slightly lower assay values were noted for F4 (92.70 and 92.96%), they remained within acceptable pharmacopeial limits and showed no indication of degradation. Across all formulations, assay values remained within a narrow range of 92.7% to 99.1%, demonstrating high chemical stability despite repeated thermal exposure. There is no degradation, nor new impurities were found after ten reuse cycles for all formulations and laser speeds. These findings improved the sustainability and cost-effectiveness of pharmaceutical SLS manufacturing by showing that these powder blends may be reused without losing the drug integrity.

Journal Pre-proof

3.4 Differential Scanning Calorimetry

The thermal analysis of all samples was performed to confirm the absence of crystallinity in both the physical mixture and the 3D-printed tablets, as illustrated in Figure 4 (A1-A5). The differential scanning calorimetry (DSC) analysis detected the melting endotherm of Indomethacin (IND) in the pure drug and the physical mixtures of F1, F2, F3, and F4 which have Kollidon® VA64 and Starch 1500®, but the F5 and F6 physical mixtures do not show any peak corresponding to the melting point (T_m = 160.4°C) of the *γ*-form of IND.

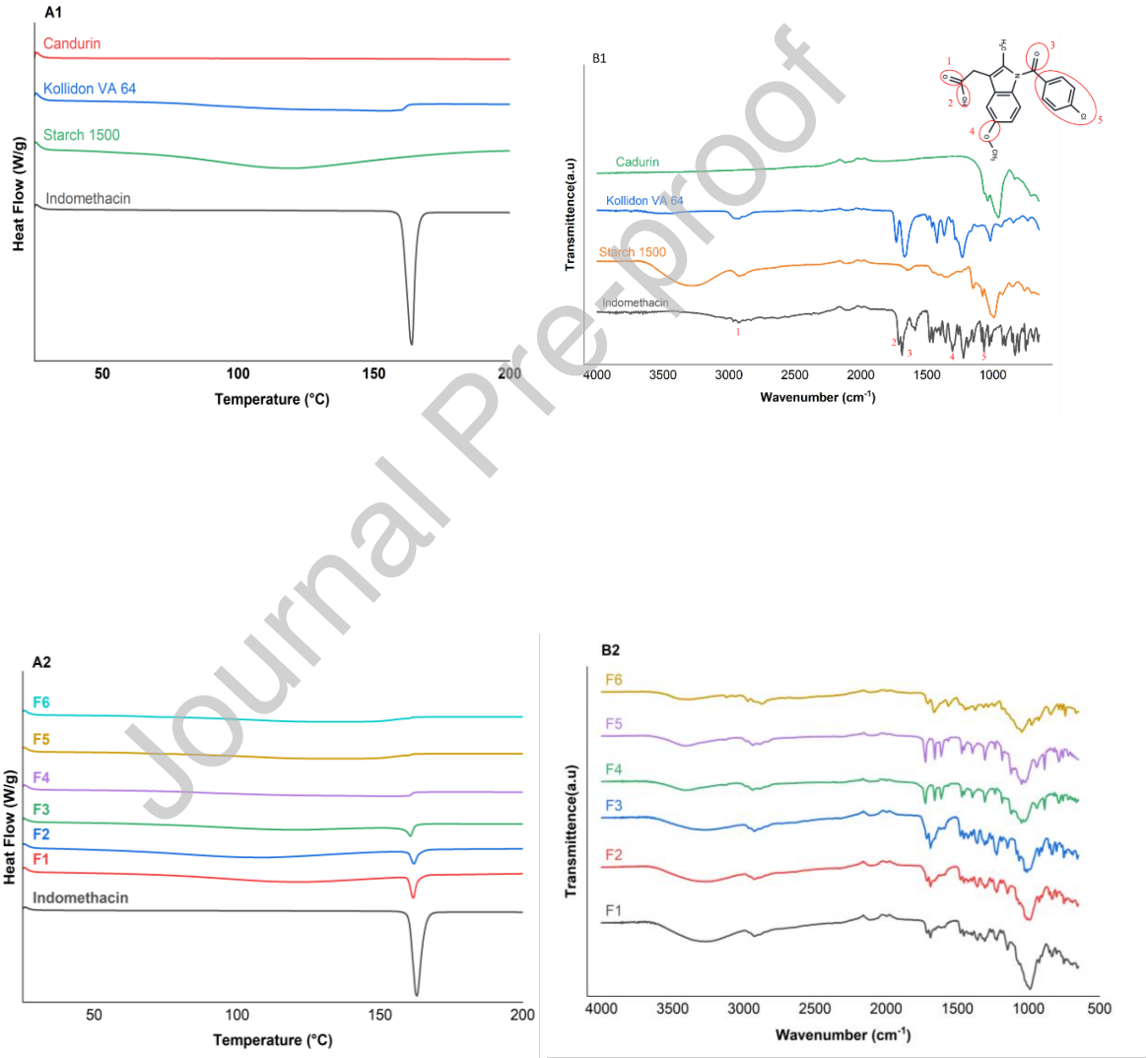

Journal Pre-proof

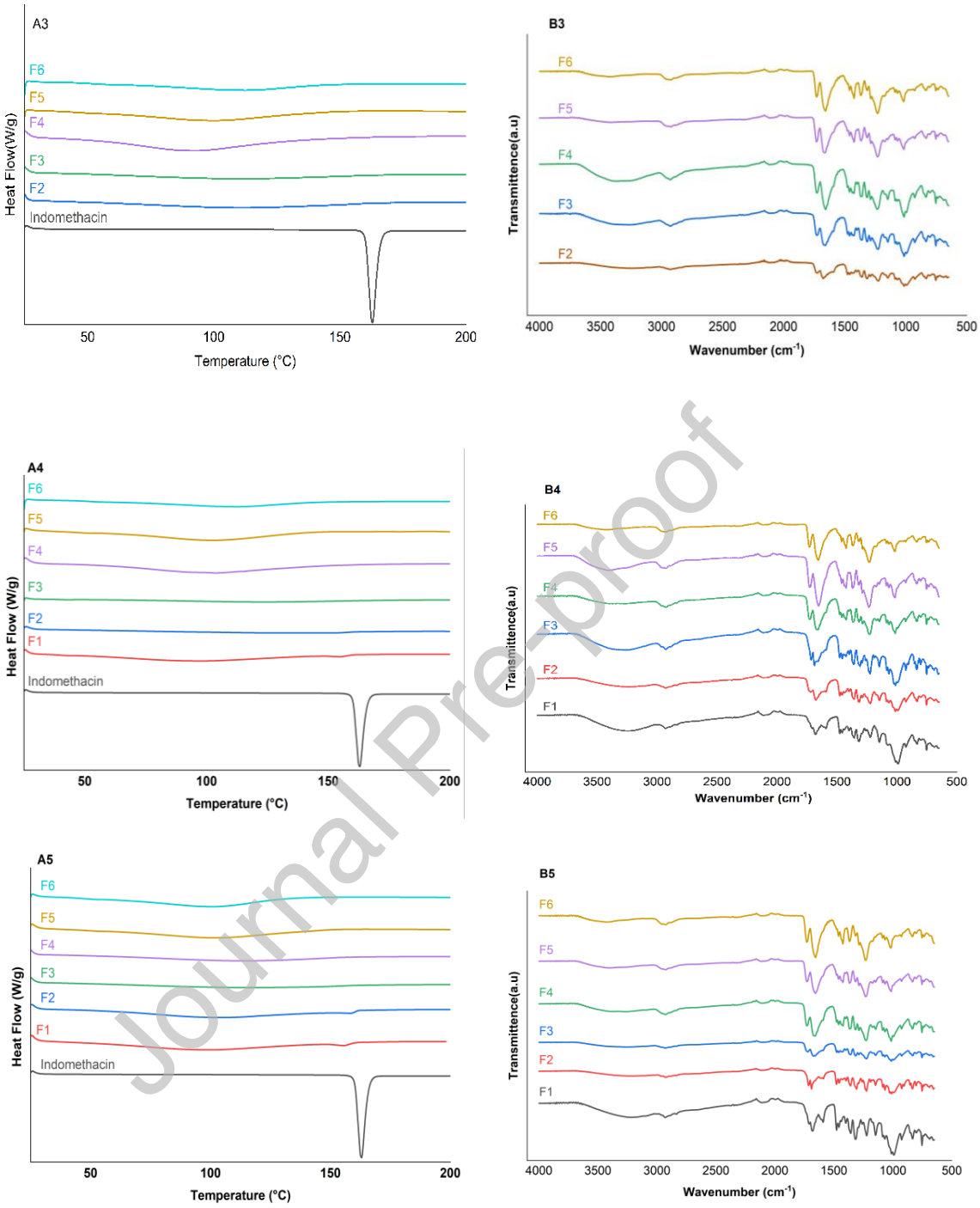

Figure 4 DSC thermograms of all A1) raw materials, A2) physical mixtures, and A3) printed formulations with LS 200 mm/s, A4) LS 250 mm/s, A5) LS 300 mm/s, and FTIR spectra for B1) all raw materials, B2) physical mixtures and B3) printed formulations with LS 200 mm/s B4) LS 250 mm/s B5) LS 300 mm/s.

Journal Pre-proof

These findings from Figure 4 DSC thermograms indicated drug amorphization within all the printed formulations of F1, F2, F3, F5, and F6 tablets, with laser speeds of 200, 250, and 300 mm/s**.** The absence of drug crystallinity in the DSC thermogram for Kollidon® VA64 powders can be attributed to the possible dissolution of IND particles within the polymer structure because of heating during analysis. At the same time, a slight degree of crystallinity was detected in the F1-300 printed tablets, which contain only Starch 1500® as an excipient.

FTIR analysis of all samples offered additional insights into the interactions between IND and other components in the formulation. The FTIR spectra of IND displayed characteristic peaks at 2926.6 cm^{-1} (O-H stretching vibration), 1717.0 cm^{-1} (C=O stretching of the carboxylic acid dimer), 1691.5 cm^{-1} (C=O stretching of the benzoyl group), 1307.7 cm^{-1} (C–O), and 1068.0 cm^{-1} (C–Cl), as shown in Figure 4 (B1-B5). Typically, carbonyl groups of amides (where nitrogen atoms are present) show peaks at wavenumbers around 1640 cm^{-1} (Garbacz & Wesolowski, 2018). However, since it's an indole ketone in IND and the nitrogen is part of the ring structure, the mesomeric effect (where nitrogen donates its lone electrons) is reduced. This explains the higher wavenumber observed for the benzoyl group in the γ-form (Ewing et al., 2014). The 1717.0 cm^{-1} peak is related to the formation of a carboxylic acid cyclic dimer, where hydrogen bonds form between two carboxylic acid groups that are not sterically hindered (Taylor & Zografi, 1997a). These dimers are important for IND's stability and for its re-crystallization after it changes from an amorphous state. The fact that peaks 2 and 3 remain present in all the samples suggests that IND did not undergo chemical degradation or react undesirably with any excipients. The changes observed in the peaks after processing are expected due to the drug's conversion into an amorphous form. After this conversion, the benzoyl carbonyl peak shifted from 1691 cm^{-1} to 1684 cm^{-1}, consistent with the crystalline γ-form, where the carbonyl group is stabilized by hydrogen bonding with the hydroxyl group of a neighboring IND molecule. Additionally, the carboxylic acid dimer peak shifted from 1717.0 cm^{-1} to 1733.0 cm^{-1}. Previous researchers indicate that after amorphous conversion, IND exists as either cyclic dimers (around 1706 cm^{-1}) or non-hydrogen-bonded carboxylic acid (around 1735 cm^{-1}) (Ewing et al., 2014; Thakkar, Zhang, et al., 2021). The FT-IR spectra of the 3D printed tablets did not show strong drug peaks due to the Kollidon® VA64 and starch® 1500 overshadowing the drug peaks, and it was expected that the drug and polymer would form an amorphous solid dispersion after processing.

3.5 Powder X-ray diffraction (pXRD)

The XRD analysis of IND, excipients, physical mixtures, and all the formulations are illustrated in Figure 5 and Figure S5.2. The diffractogram of pure IND exhibits distinct peaks observed in Figure S1 at 11.5, 19.4, and 21.7 two-theta (2θ) degrees, which comply with previous reports. Similarly, the diffractograms of the physical mixtures retained these characteristic peaks of the drug, with

a noticeable reduction in the peaks' intensity. In contrast, the formulations displayed a broad halo, signifying the disappearance of all the peaks. Further, there are two small peaks at 19.8 and 25.2 2θ degrees, out of which one overlaps with the characteristic peak of IND at 19.4 2θ degrees. These peaks belong to Candurin, which is the photo-absorbing species required for the successful sintering and hence should not be confused with the presence of trace crystallinity in the SLS 3D printed tablets (Davis et al., 2020; Davis Jr. et al., 2020). This can further be proven by the DSC results depicted in Figure 5. This XRD data complements the findings from the DSC analysis and confirms the transformation of the crystalline drug into its amorphous form upon interaction with the polymers during the sintering process.

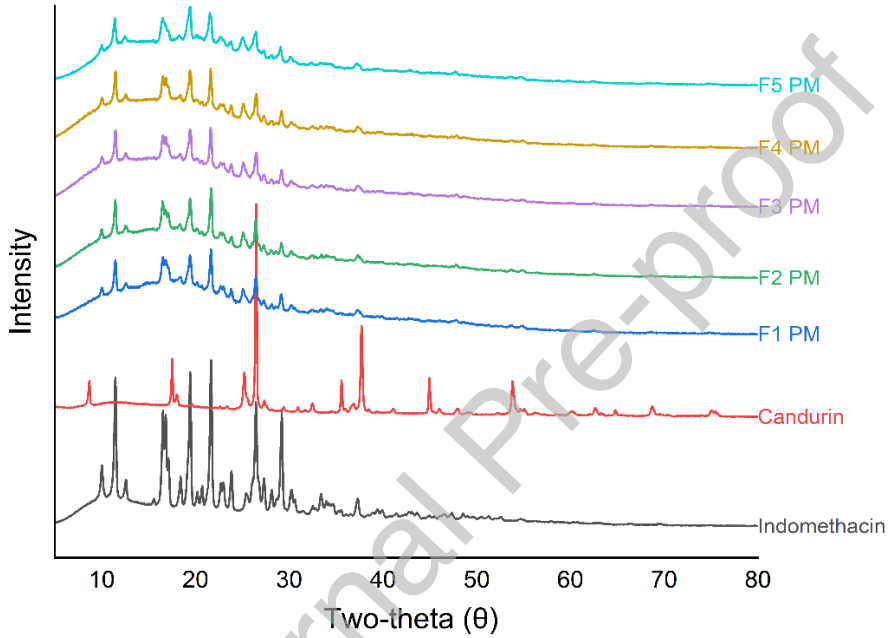

Journal Pre-proof

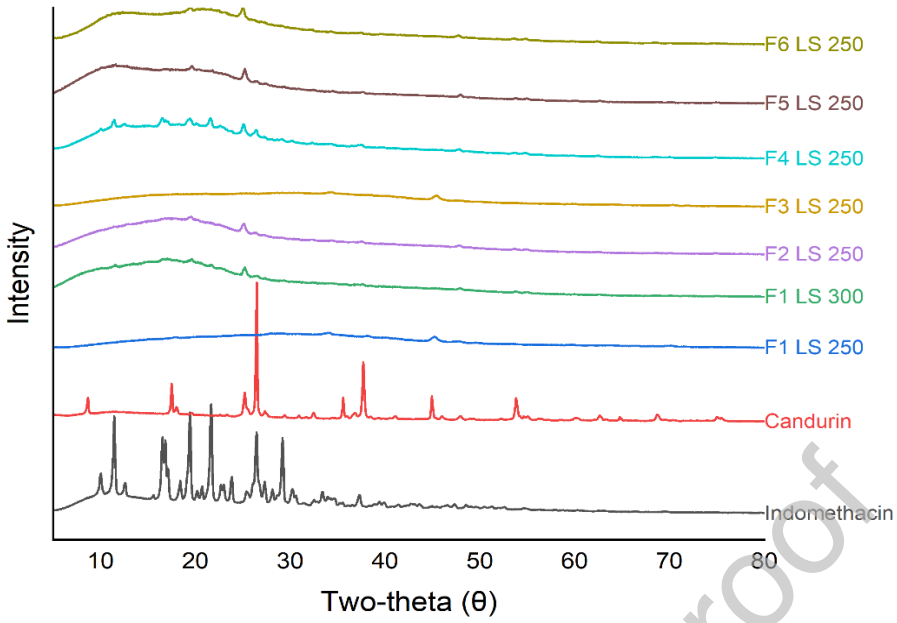

Figure 5 Powder X-ray diffraction for Pure Indomethacin, Candurin® gold sheen, Physical mixture (F1- F5), and 3d printed tablets with LS 250 mm/s (F1-F6), confirming amorphous conversion of the drug

3.6 ^{1}H-NMR spectroscopy

The structural integrity and chemical compatibility of Indomethacin with the selected excipients employed in powder bed fusion by selective laser sintering (SLS) were evaluated using proton nuclear magnetic resonance (^{1}H-NMR) spectroscopy (400 MHz, DMSO-d_6). Comparative spectra were obtained for the pure drug and its 3D-printed formulations (F1–F6), processed at laser speeds of 200, 250, and 300 mm/s, to assess potential interactions and confirm the preservation of the drug's molecular framework, depicted in Figure 6. The chemical shifts are denoted in Table S4.3, Table S4.4 and the 1H NMR spectroscopies of the excipients are shown in Figure S5.3.

Journal Pre-proof

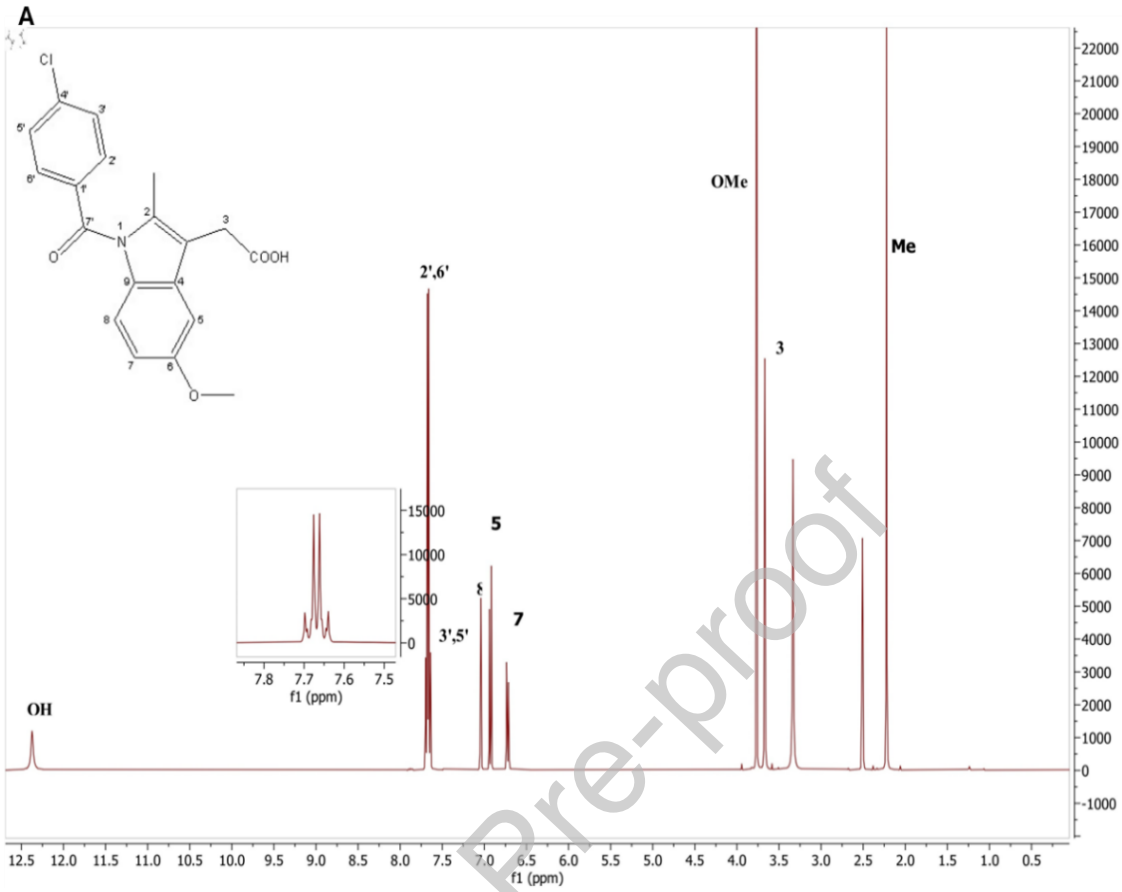

Journal Pre-proof

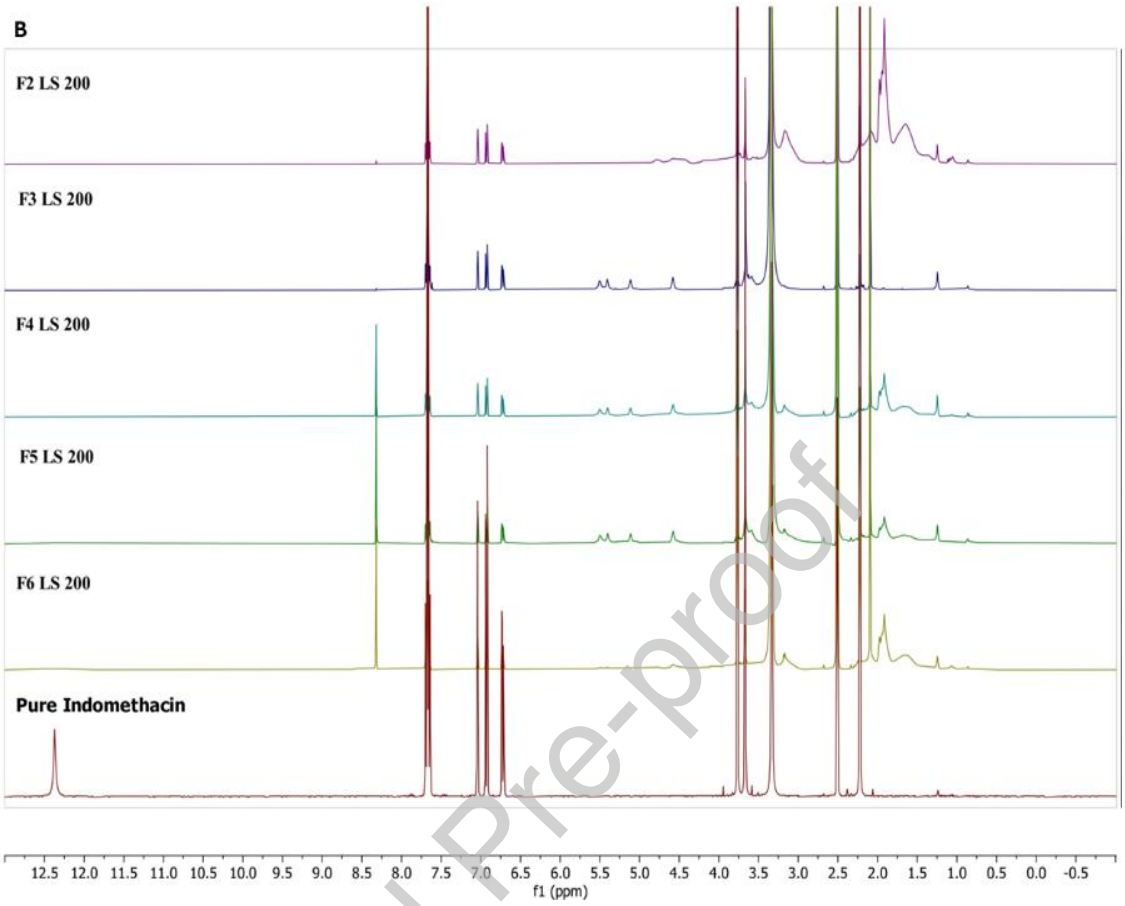

Journal Pre-proof

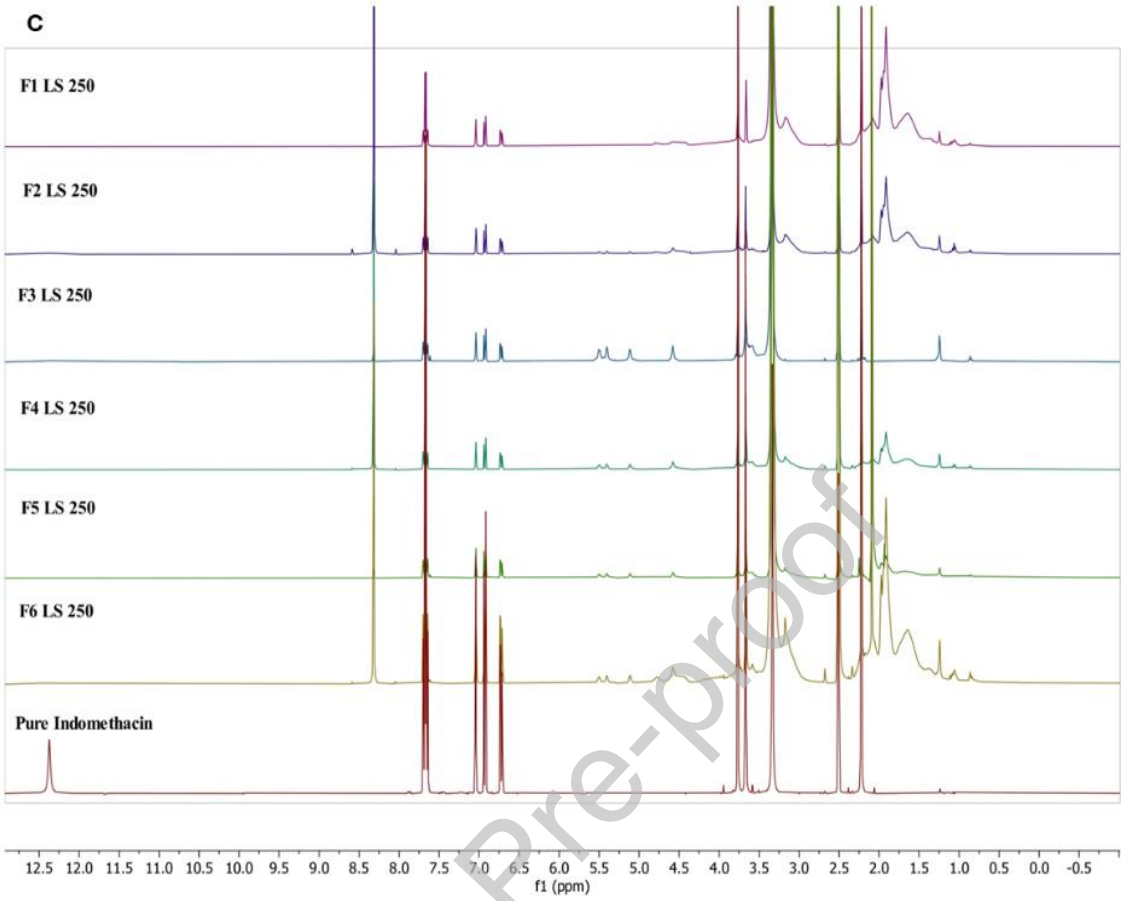

Journal Pre-proof

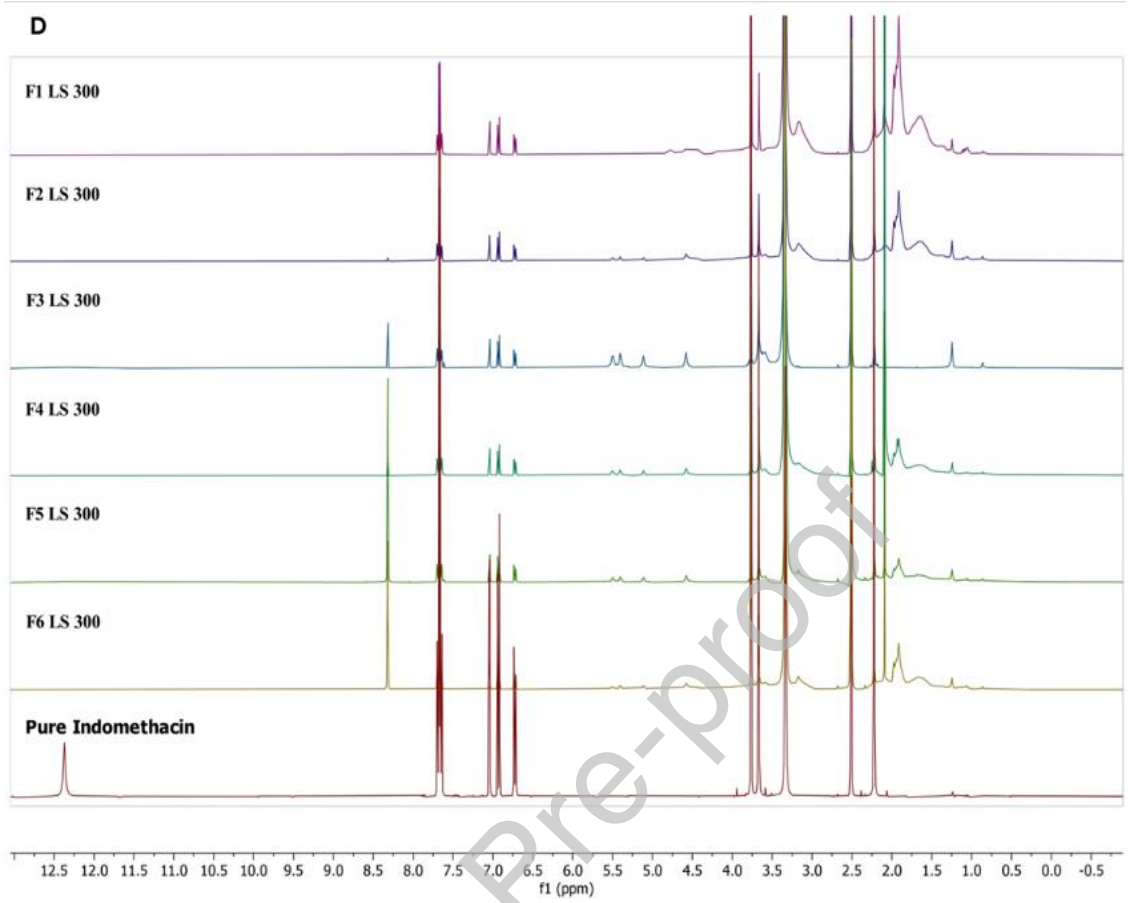

Figure 6 A) ^{1}H NMR overlay spectra of Pure Indomethacin in DMSO-d_6, B) 3D printed formulations (F2–F6) processed at laser scanning speeds (200 mm/s), C) F1-F6 processed at laser scanning speed 250 mm/s, D) F1-F6 processed at laser scanning speeds with 300 mm/s, confirming preservation of chemical structure after laser sintering.

The reference spectrum of pure Indomethacin revealed key diagnostic resonances consistent with its structure. A highly downfield singlet at δ 12.39 ppm corresponds to the carboxylic acid proton, indicative of intramolecular hydrogen bonding. A complex multiple between δ 7.70 and 7.63 ppm (integrating for four protons) represents the overlapping aromatic protons from the indole and benzoyl rings. A set of aromatic doublets and a doublet of doublets at δ 7.04, 6.93, and 6.72 ppm reflect a trisubstituted aromatic ring system with ortho- and meta-couplings. A singlet at δ 3.77 ppm corresponds to a methoxy (-OCH_3) group, while another singlet at δ 3.67 ppm (2H) is assigned to a methylene (-CH_2) group adjacent to an electronegative center. A broad singlet at δ 3.35 ppm integrating for ~7H may include excipient-related methylene or methoxy groups. The singlet at δ 2.22 ppm (3H) is characteristic of a methyl (-CH_3) group bonded to an aromatic system.

Overlay analysis of the printed formulations (F1–F6) showed no chemical shifts, additional peaks, or signal broadening, indicating no degradation or interaction between Indomethacin and the excipients under any processing condition. The carboxylic acid and aromatic proton signals remained unchanged, confirming chemical integrity post-processing. Formulations F1–F3 and F5–F6 incorporated Kollidon® VA64 as the primary matrix former, whereas F4 used Starch 1500® alone. The lack of any new or missing peaks in these formulations supports that both Kollidon® VA64 and Starch 1500® are chemically inert under the SLS conditions applied. Thus, these results affirm that neither elevated surface/chamber temperatures nor increased laser energy input compromised drug stability, even in formulations with starch-only matrices. The excipients did not undergo detectable chemical interactions with the API.

3.7 HPLC Analytical Method and Validation

The RP-HPLC method exhibited excellent performance across all validation parameters. The retention time was about 6.2 minutes, effectively maintaining the sharpness of the Indomethacin peak depicted in Figure 7 . All the results are described in supplementary results S3, Supplementary tables S4 and Figures S5

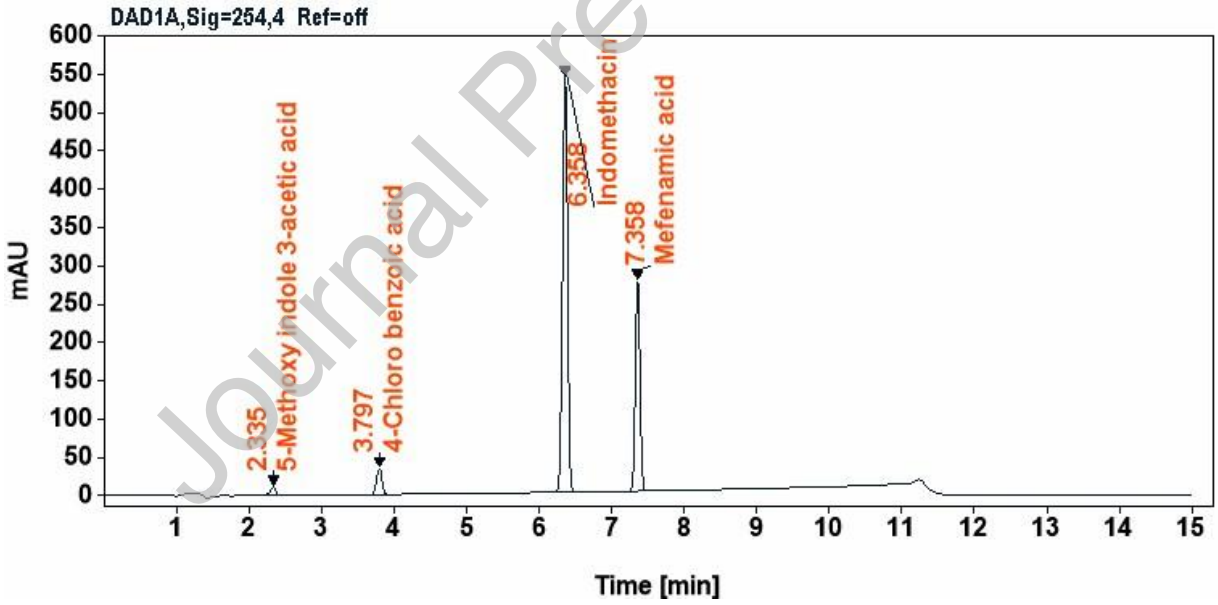

Figure 7 Chromatogram indicating the clear separation of degradants, indomethacin, and internal standard at detection wavelength 254 nm.

Journal Pre-proof

3.8 Drug Content

The drug content was quantified to determine any drug loss due to laser exposure during the printing process. The results indicated that the drug content for all the formulations was within the range of 97.9 to 105.2, as listed in Table 4 which is within the acceptable limits of 90 to 110%.

Table 4 Drug Content for all SLS 3DP tablets with different Laser speeds.

Formulation Code	Average Content Uniformity (%) ± Standard deviation (SD)		
	LS 200 mm/S	LS 250 mm/s	LS 300 mm/s
F1	N/A	97.9 ± 4.22	99.6 ± 4.22
F2	100.4 ± 0.58	104.7 ± 3.63	104.7 ± 3.63
F3	101.8 ± 1.03	102.5 ± 3.87	102.5 ± 3.87
F4	104.3 ± 1.55	98.2 ± 4.06	105.2 ± 5.06
F5	104.8 ± 1.35	100.3 ± 2.06	100.3 ± 2.06
F6	102.6 ± 1.16	100.2 ± 3.81	100.2 ± 3.81

The Low variability (SD ≤ 5.06) across all formulations demonstrates consistent drug distribution and limited effect of laser processing on drug content with no statistically significant differences across formulations.

3.9 *In vitro* release testing

The dissolution *In vitro* used a pH-shift procedure instead of the USP pH 7.2 buffer to mimic physiological conditions. Following 750 mL of 0.1 N HCl (pH 1.2), samples were placed in 1000 mL of phosphate buffer (pH 6.8). IND is a weakly acidic compound (pKa 4.5) with poor water solubility, primarily due to its hydrophobic indole group. In acidic environments, IND is insoluble, with a solubility of 7-9 µg/mL, but becomes soluble when ionized at higher pH. Laser-sintered formulations must evaluate dissolution under the pH-transit protocol because IND is amorphous, which has a higher chemical potential and faster dissolution than its crystalline form, but is more unstable and recrystallizes in acidic environments. Exposing formulations to acidic conditions first ensures physiologically appropriate assessment and identifies recrystallization hazards that could hinder *in vivo* performance. This study additionally investigated how the concentration of the excipient and the speed of the laser affected the results. Kollidon®VA64, Starch 1500®, and a combination of the two were evaluated. The drug was amorphous in all Starch 1500® and Kollidon® VA64 formulations.

When exposed at pH 1.2 for 2 hours, all formulations with three laser speeds showed slight improvements in drug release, which remained below 10% for all the formulations compared to negligible release from the crystalline pure drug depicted in Figure 8, indicating modest improvement due to amorphization. However, significant differences emerged after pH

transition. This enhancement may be attributed to the drug's amorphous state during sintering and the presence of binders Starch 1500® and Kollidon® VA64. Formulation F1 (200 mm/s) was unsuccessful because the laser exposed Starch 1500® for too long, resulting in a defective printlet. At a 200 mm/s laser speed, formulation F6 released 5.5% at 2 h, followed by F3, F5, and F4. Increasing the laser speed to 250 mm/s improved acidic-phase dissolving, with F6 (Kollidon® VA64 rich) again performing best at 7.5%, F1, F2, F3 showing only slight improvement, and F4, F5 showing substantial enhancement compared to the crystalline drug. The release profiles showed minor changes at 300 mm/s, due to partial recrystallization or precipitation. However, filtering over a 0.2 µm membrane demonstrated that dissolution outpaced recrystallization, resulting in greater drug concentrations at 120 min. Overall, Figure 8 and Figure 9 show that all printed formulations had better acidic-phase release than the crystalline API due to increased Kollidon® VA64 concentration and lower Starch 1500® levels over 2 h.

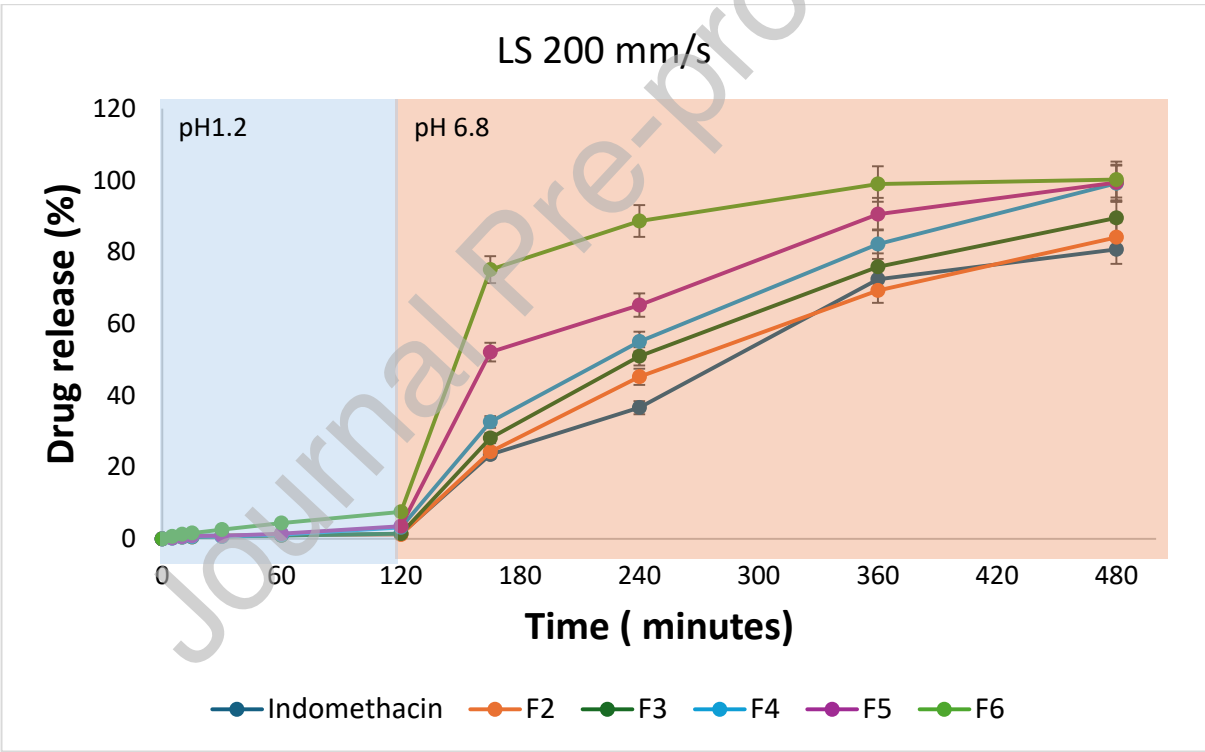

Journal Pre-proof

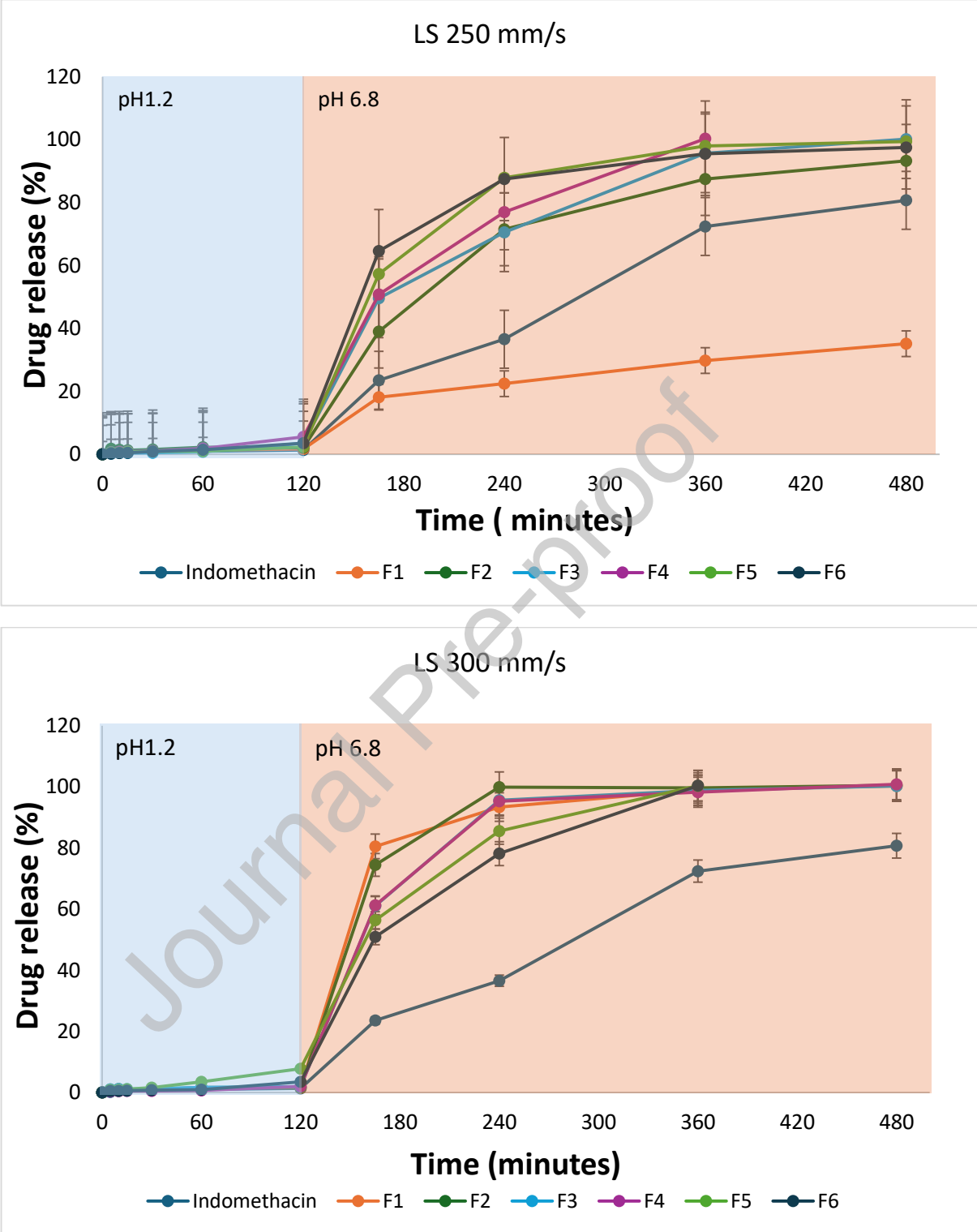

Figure 8 pH shift dissolution of printed formulations using laser speeds 200 mm/s, 250 mm/s, and 300 mm/s.

Journal Pre-proof

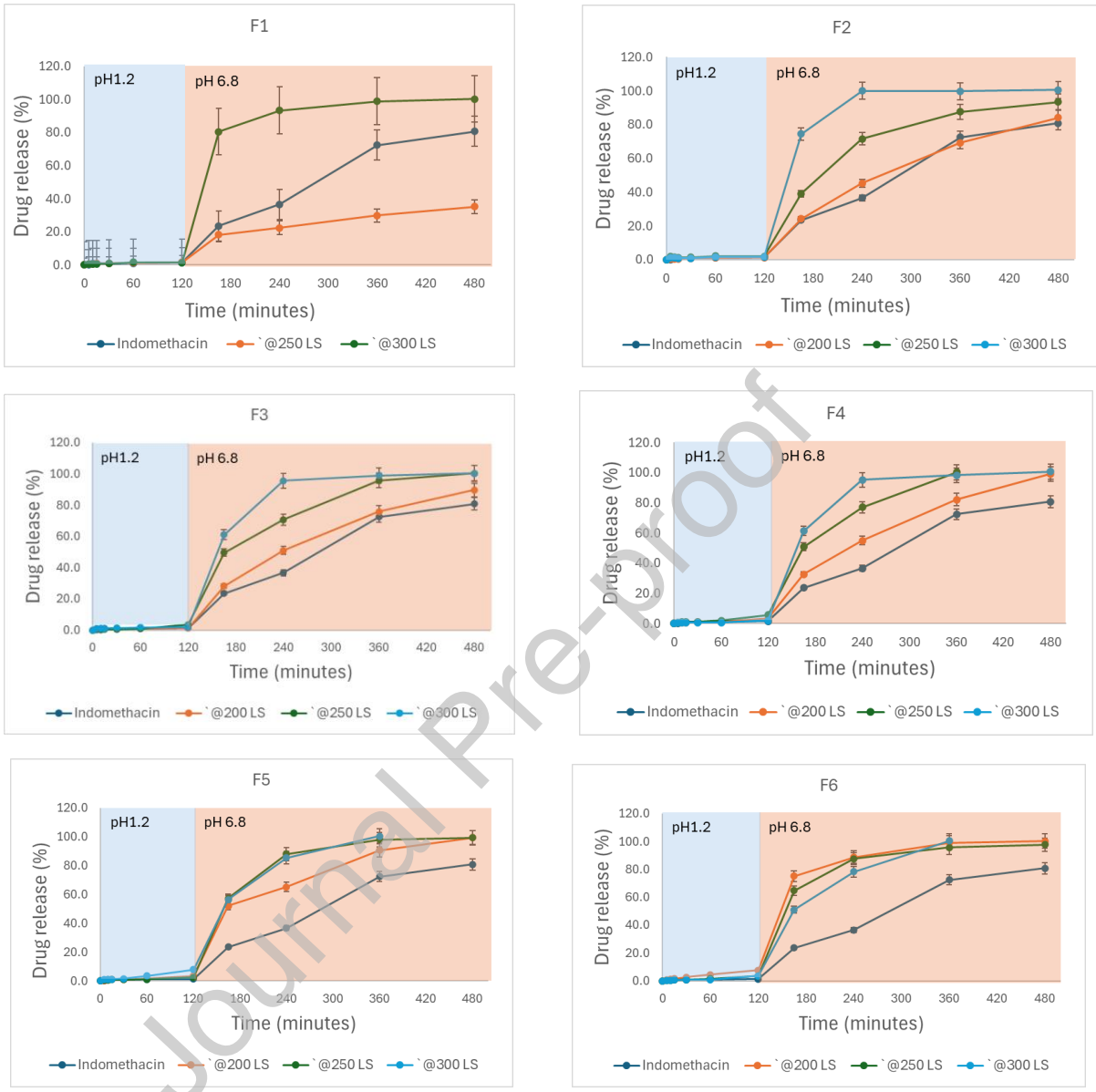

Figure 9 pH shift dissolution comparison of F1-F6 formulation in all laser speeds vs Pure API

Journal Pre-proof

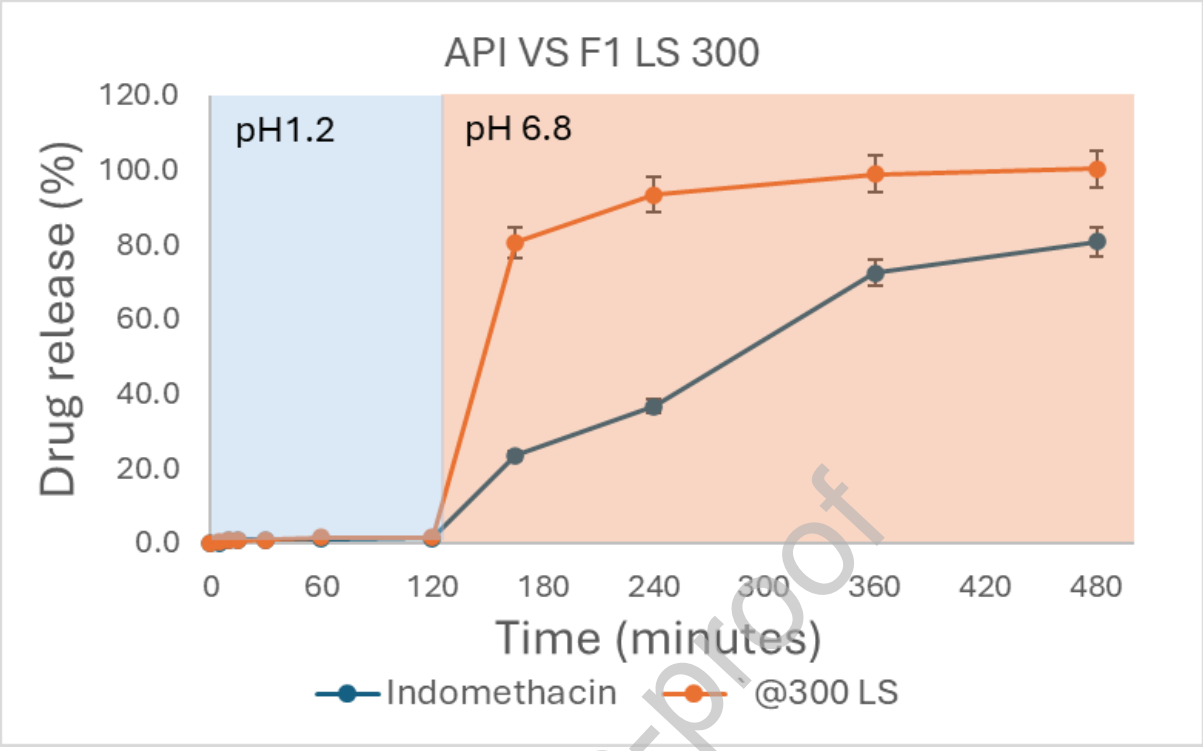

Figure 10 pH shift dissolution of F1 LS 300 mm/s Lead formulation vs Pure API

When the media shifted from pH 1.2 to pH 6.8, all the tablets demonstrated improved drug release. At a 200 mm/s laser speed, F6 formulation showed 95% release, followed by other formulations, which released more than 70%, compared to crystalline API, which released only 36.6% within 2 hours of pH shift. When dissolution studies at a 250 mm/s laser speed were investigated, drug release was more than 84% for all formulations except for F1 (35.2%), whereas at a 300 mm/s LS, drug released was 100% within 6 hours for all the formulations, here F1 300 mm/s containing only sole starch 1500® was considered as a lead formulation, showed 80% release in 45 mins after pH shift when compared to 23% release of crystalline pure API, as illustrated in Figure 10, representing more than a three-fold enhancement.

In wet-processed tablets, pregelatinized starch usually creates thick gel layers that delay drug release; therefore, the quick dissolving attained by starch-only formulations, especially F1 at 300 mm/s, was surprising (Eraga et al., 2024; Hong et al., 2016; Thiptinnakorn et al., 2020; Zamboulis et al., 2022). The content uniformity of the tablets was within the acceptable range, as reported in section 3.8 The dissolution profiles of the SLS 3D printed tablets peaked at 100% drug release (6 hours after the pH shift), except for F1 (250 mm/s). This enhanced drug release can be attributed to the formation of amorphous solid dispersions (ASDs) stabilized by Starch 1500® and Kollidon® VA64 during the SLS 3D printing process. Also, correlates to the porosity microstructure observed in SEM imaging, especially in starch-rich formulations.

Journal Pre-proof

These ASDs serve as supersaturating drug delivery systems, where the polymer matrix stabilizes the drug and maintains supersaturation through intermolecular interactions. Overall, the starch-rich formulations consistently demonstrated faster drug release compared to polymer-rich systems, highlighting that the matrix composition has a predominant influence on the dissolution kinetics.

4 Discussion

The present study is the first to investigate the application of Starch 1500®, a partially pregelatinized maize starch, as a sole excipient in Selective Laser Sintering (SLS) 3D printing for the formulation of Indomethacin (IND) oral tablets. To the best of our knowledge, this is the first report evaluating the printability, sintering behavior, and dissolution performance of Starch 1500®, a green excipient under SLS 3DP processing conditions. Traditional powder-bed-based 3D printing systems often rely on synthetic polymers or require excipient blends to achieve robust printing and effective drug release. We hypothesized that the unique partial gelatinization, high amylopectin fragmentation, and inherent moisture-binding capacity of Starch 1500® would facilitate its direct use in SLS 3D printing technology without the need for additional solubilizers, disintegrants, and binders, enabling robust sintering and simultaneously enhancing the dissolution of indomethacin (IND), a poorly soluble and thermolabile model drug. Furthermore, we anticipated that combining Starch 1500® with Kollidon® VA64 would yield synergistic performance by pairing starch's diffusion-controlled hydration and erosion with the polymer's supersaturation-stabilizing effect, thereby optimizing release profiles across gastrointestinal pH conditions. Thus, this study demonstrates that Starch 1500® alone can produce structurally sound, defect-free tablets capable of enhancing the dissolution of poorly soluble drugs.

Commercial Starch 1500® contains ~5–15% residual crystallinity, an amylopectin content exceeding 80%, and a median particle size (D50) of 40–60 µm, with low water activity (<0.3 aw) despite a total moisture content of 10–14% (Ai & Jane, 2015; Sheng, 2009a). This dual-phase structure features fragmented amylopectin chains interspersed with crystalline lamellae, providing a balance between thermal plasticity and particle rigidity. Under SLS conditions, the amorphous regions soften and fuse under localized heating, while crystalline remnants preserve particle morphology during powder spreading. This explains the excellent flow properties observed and the defect-free layer deposition, which are critical for uniform sintering in powder-bed systems (Damiri et al., 2025; Zamboulis et al., 2022).

The processing performance of Starch 1500® under SLS conditions can be directly attributed to its molecular and supramolecular structure. The fragmented amylopectin chains and reduced crystallinity lower the glass transition temperature, enabling sintering and interparticle bonding at surface temperatures as low as 105 °C and laser speeds of 200–300 mm/s, well below the

degradation threshold of IND (Tm ≈ 160°C). Unlike conventional wet granulation or direct compression, where pregelatinized starch often forms viscous gel layers that slow drug release (Hong et al., 2016; Thiptinnakorn et al., 2020) (Michailova et al., 2001). However, in the SLS-printed matrix, the combination of localized heating and rapid solidification alters the molecular organization of the starch, disrupting amylopectin chain entanglement and suppressing retrogradation, thus facilitating water ingress and drug diffusion. The findings align with (Sheng, 2009a).

Indomethacin and other poorly water-soluble drugs have commonly been explored using material extrusion-based 3D printing to enhance their solubility and streamline dosage form manufacturing (Viidik et al., 2021; Xu et al., 2020). Polymers such as polycaprolactone and hydroxypropyl methylcellulose have been processed into filaments specifically for this purpose. However, high processing temperatures inherent in filament deposition methods can degrade thermally sensitive drugs like indomethacin by exceeding their melting points (approximately 160°C) (Shimada et al., 2018). To circumvent this limitation, powder bed-based additive manufacturing techniques, including binder jetting and selective laser sintering (SLS), have emerged as superior alternatives (Fina et al., 2017b). These methods offer significantly lower surface temperatures, reducing the risk of thermal degradation without necessitating plasticizers. Particularly, SLS has garnered attention for fabricating porous drug structures and has been demonstrated to be effective for various pharmaceuticals, such as levetiracetam (Petruševska et al., 2015), acetaminophen (Fina et al., 2017c), and ritonavir, facilitating amorphous solid dispersion formation to improve solubility substantially (Davis Jr et al., 2021, p. 3).

The optimized SLS process preserved indomethacin stability while enhancing dissolution compared to the crystalline drug. Unlike conventional solid dispersion techniques that rely on solvents and precipitation inhibitors such as hydroxypropyl methylcellulose (HPMC) and Kollicoat® IR (Y. Li et al., 2019; Majumder et al., 2018; Xi et al., 2020a), this solvent-free SLS approach exploits the intrinsic functionality of Starch 1500®, either alone or in combination with Kollidon® VA64. Our findings reveal these polymers significant roles in stabilizing the amorphous state of indomethacin by inhibiting recrystallization (Kosaka et al., 2020). Starch 1500® improved wettability, binding, and limited molecular mobility through hydrogen bonding, and functioned as a moisture scavenger by binding water at low activity, thereby suppressing moisture-induced recrystallization and promoting rapid hydration and disintegration, and letting drugs be released quickly without being limited by diffusion (Sheng, 2009b). Kollidon® VA64 further stabilized the amorphous drug and maintained supersaturation, thereby preventing recrystallization (Mohapatra et al., 2017), although higher polymer levels formed denser matrices that slowed release via diffusion control. These results are consistent with prior studies where VA64 has been used to facilitate drug dispersion and stabilize amorphous APIs in 3D printing (Sridhar, 2013; Strojewski & Krupa, 2022; Szafraniec-Szczęsny et al., 2021; Tres et al., 2016). On the other hand,

Thakkar, Zhang, et al. (2021) used a DosePlus system that combined hot-melt granulation and SLS with polysorbate 80 and Kollidon® VA64 for the rapid dissolution of indomethacin.

Dissolution enhancement was primarily due to complete amorphization during SLS, as confirmed by DSC and PXRD, together with laser-speed-dependent changes and composition-dependent differences in porosity and surface area. Higher scan speeds (300 mm s^{-1}) generated more open pore networks that facilitated rapid liquid penetration, starch swelling, and fast tablet breakup, whereas lower speeds produced denser structures that delayed release. Scanning electron microscopy (SEM) examination gave direct insight into the microstructural changes between formulations and their significance in influencing drug release behavior. The starch-rich formulations (F1–F3) revealed a very porous and heterogeneous structure, with irregular fused particles and evident interparticle spaces. The limited thermoplastic flow of the partially pregelatinized starch during sintering caused not perfect coalescence and pore development, resulting in an open network. On the other hand, formulations with higher proportions of Kollidon® VA64 (F4–F6) showed a more homogeneous and compact matrices with lower porosity, which suggests better interparticle fusion due to the thermoplastic character of the polymer. These variances demonstrate that the microstructure is mostly determined by the content of the formulation, not only by the processing parameters in the case of SLS-printed tablets. These morphological variations are directly related to the observed dissolution behavior. The porous structure of starch-rich formulations leads to quick penetration of solvents and therefore faster hydration, swelling and drug diffusion. In contrast, in polymer-rich systems, dense matrices inhibit solvent penetration and generate diffusion-controlled pathways, leading to a comparably slower rate of drug release.

The findings of the density and porosity demonstrate that the interior structure of SLS 3D printed tablets is highly affected by both the formulation composition and the laser speed. The density increased and the porosity decreased with the larger polymer content (F1→F6), indicating creation of a more compact matrix. Similarly, lower laser speed (LS 200) created denser tablet with higher energy input and better particle fusion, whereas higher laser speed (LS 300) led in more porous structures. The structural changes thus obtained are directly related to the mechanical strength and are expected to influence the drug release. The porous tablets promote a rapid penetration of the liquid and a faster release, while the denser matrices favor a diffusion-controlled release.

Under pH-transit conditions, crystalline indomethacin released slowly, while the starch-rich formulation F1 printed at 300 mm/s achieved 80% release within 45 min after the pH shift, as depicted in Figure 10, demonstrating an optimal balance between minimal gastric release and rapid intestinal onset. Comparable dissolution to surfactant-assisted systems was achieved

without solubilizers, highlighting the effectiveness of starch-based SLS formulations for enhancing the performance of poorly soluble drugs.

The FTIR spectra from Figure 4 revealed distinct changes in the carbonyl stretching peak at 1717 cm^{-1}, which showed broadening and reduction due to strong hydrogen bonding, or intermolecular interactions between IND and excipients, which was already reported by (Taylor & Zografi, 1997b; Xi et al., 2020b) (Hasegawa et al., 2024). Additionally, PXRD patterns and DSC thermograms demonstrate complete amorphous conversion during sintering, supporting earlier heat-based printing experiments (Kollamaram et al., 2018). ^{1}H-NMR spectra findings from Figure 6 revealed that SLS processing conditions did not compromise the molecular integrity of API.

The powder flow properties and blend uniformity were also critical for the SLS process. Prior research has highlighted the importance of excipient flow in SLS 3DP, especially for hydrophilic excipients with poor flow characteristics (Norman et al., 2017). Starch 1500®'s performance in this regard establishes it as a functional candidate for powder bed systems.

In the broader context of polysaccharide research, our findings expand the role of starch-based excipients in advanced manufacturing. This study demonstrates that a single, minimally processed carbohydrate polymer can provide mechanical integrity for SLS powder-bed printing and effective dissolution enhancement. Previous carbohydrate polymer studies in 3DP have often relied on cellulose derivatives (Cardoso & Araújo, 2024; Giri et al., 2021), chitosan (J. Li et al., 2025; Maliki et al., 2022), or dextrins (Aguilar-de-Leyva et al., 2020; Lam et al., 2002; Zamboulis et al., 2022), often relying on solvent-based processing or multi-polymer blends to ensure printability and drug release. This shows that Starch 1500® is a sustainable, pharmaceutically acceptable excipient that can serve as a unique matrix in SLS 3DP. Collectively, these findings suggest starch-based SLS 3DP as a long-lasting, solvent-free, and excipient-free way to make pharmaceuticals that do not dissolve well, but dissolve better. More research is needed to look at more APIs and polymers to see if this method can be used on a larger scale.

5 Conclusions

Starch 1500® served as a single, pharmaceutically accepted excipient enabling solvent-free, selective-laser-sintered oral tablets. Localized heating and rapid cooling induced in-situ amorphization of indomethacin and suppressed retrogradation, producing improved drug release without surfactants. Binary Starch 1500® and Kollidon® VA64 formulations stabilized supersaturation while maintaining tablet integrity. This sustainable, excipient-minimal strategy demonstrates how carbohydrate polymers can power additive manufacturing for future patient-specific dosage forms.

CRediT authorship contribution statement.

Sujith raj Bashetty: Writing - original draft, Writing - review & editing, Visualization, Software, Validation, Methodology, Investigation, Formal analysis, Data curation, Conceptualization. Yu Zhang: Writing- original draft, review & editing, Formal analysis, Data curation, Conceptualization. Navya Nalajala: Methodology, Formal analysis, Data curation. Thirupathi Anekalla: Methodology, Data curation, Validation. Lakshmi Priyanka: Visualization, review & editing. Nagarjuna Narala: Investigation, Formal analysis, Data curation. Rohith Alluri: Formal analysis, Data curation. Mohammed Maniruzzaman: Writing - review & editing, Supervision, Resources, Project administration, Investigation, Funding acquisition.

Declaration of Competing Interest

The authors declare that they have no known competing financial interests or personal relationships that could have appeared to influence the work reported in this paper.

Acknowledgments

The authors acknowledge the generous support provided by Colorcon (Indianapolis, USA) with Starch 1500 and technical guidance from Ali Rajabi-Siahboomi, Shahrzad Missaghi and Russell Prestipino. The PharmE3D lab, Pharmaceutics and Drug Delivery, University of Mississippi, financially supported this work. The authors thank the support of Sitalu Karumutchu and Kumar Katragunta for Instrumental Analysis, School of Pharmacy, University of Mississippi.

Declaration of generative AI use

If any AI tools were utilized, this would have been solely to assist with language refinement, grammatical correction, and readability improvement when writing this publication. The AI tool did not create scientific material, analyze data, plan experiments, or conclude. All scientific content, data interpretation, and findings are created by the authors who read and edited the work and accept full responsibility for its integrity and correctness.

Data availability

Data will be made available on request.

Journal Pre-proof

References

Aghajani M, Garshasbi HR, Naghib SM, Mozafari MR. 3D printing of hydrogel polysaccharides for biomedical applications: a review. Biomedicines. 2025 Mar 17;13(3):731.

21 CFR 73.3128. (2024, October). *21 CFR 73.3128—Mica-based pearlescent pigments.* https://www.ecfr.gov/current/title-21/part-73/section-73.3128

Aghajani, M., Garshasbi, H. R., Naghib, S. M., & Mozafari, M. R. (2025). 3D printing of hydrogel polysaccharides for biomedical applications: A review. *Biomedicines*, *13*(3), 731.

Aguilar-de-Leyva, Á., Linares, V., Casas, M., & Caraballo, I. (2020). 3D printed drug delivery systems based on natural products. *Pharmaceutics*, *12*(7), 620.

Ai, Y., & Jane, J. (2015). Gelatinization and rheological properties of starch. *Starch-Stärke*, *67*(3–4), 213–224.

Anastasiades, A., Thanou, S., Loulis, D., Stapatoris, A., & Karapantsios, T. D. (2002). Rheological and physical characterization of pregelatinized maize starches. *Journal of Food Engineering*, *52*(1), 57–66.

Angupale, J. R., Engeu, O. P., & Ignatius, O. S. (2020). Physical properties and compactability of various blends of fully gelatinised and pregelatinised maize starch. *Pharmaceutical and Biosciences Journal*, 35–44.

Balasankar, A., Anbazhakan, K., Arul, V., Mutharaian, V. N., Sriram, G., Aruchamy, K., Oh, T. H., & Ramasundaram, S. (2023). Recent advances in the production of pharmaceuticals using selective laser sintering. *Biomimetics*, *8*(4), 330.

Barakh Ali, S. F., Mohamed, E. M., Ozkan, T., Kuttolamadom, M. A., Khan, M. A., Asadi, A., & Rahman, Z. (2019). Understanding the effects of formulation and process variables on the printlets quality manufactured by selective laser sintering 3D printing. *International Journal of Pharmaceutics*, *570*, 118651. https://doi.org/10.1016/j.ijpharm.2019.118651

Bhatkande, A., Narala, S., Wang, H., Narala, N., Karnik, I., Vemula, S. K., & Repka, M. A. (2024). Extrusion-Based Three-Dimensional Printing of Metronidazole Immediate Release Tablets: Impact of Processing Parameters and in Vitro Evaluation. *Journal of Pharmaceutical Innovation*, *19*(6), 72.

Bühler, V. (2008). Kollidon. *Polyvinylpyrrolidone Excipients for the Pharmaceutical Industry*, *9*.

Cardoso, P. H. N., & Araújo, E. S. (2024). An Approach to 3D Printing Techniques, Polymer Materials, and Their Applications in the Production of Drug Delivery Systems. *Compounds*, *4*(1), 71–105. https://doi.org/10.3390/compounds4010004

Chang, H.-C., Jørgensen, B., Di Silvio, L., & Gurzawska-Comis, K. (2023). 3D bioprinted pectin-based hydrogel as sustainable biomaterials for musculoskeletal tissue engineering.

Journal Pre-proof

Sustainable Materials and Technologies, *38*, e00732. https://doi.org/10.1016/j.susmat.2023.e00732

https://www.colorcon.com/products/core-excipients/binders-dilutants-lubricants/starch-1500.2019.pdf.

Corrigan, O. I., Holohan, E. M., & Reilly, M. R. (1985). Physicochemical properties of indomethacin and related compounds co-spray dried with polyvinylpyrrolidone. *Drug Development and Industrial Pharmacy*, *11*(2–3), 677–695.

Damiri, F., Fatimi, A., Liu, Y., Musuc, A. M., Fajardo, A. R., Gowda, B. H. J., Vora, L. K., Shavandi, A., & Okoro, O. V. (2025). Recent advances in 3D bioprinted polysaccharide hydrogels for biomedical applications: A comprehensive review. *Carbohydrate Polymers*, *348*, 122845. https://doi.org/10.1016/j.carbpol.2024.122845

Davis, D. A., Miller, D. A., Su, Y., & Williams, R. O. (2020). Thermally conductive excipient expands kinetiSol® processing capabilities. *AAPS PharmSciTech*, *21*, 1–15.

Davis Jr, D. A., Miller, D. A., Su, Y., & Williams III, R. O. (2020). Thermally conductive excipient expands kinetiSol® processing capabilities. *AAPS PharmSciTech*, *21*(8), 319.

Davis Jr, D. A., Thakkar, R., Su, Y., Williams III, R. O., & Maniruzzaman, M. (2021). Selective laser sintering 3-dimensional printing as a single step process to prepare amorphous solid dispersion dosage forms for improved solubility and dissolution rate. *Journal of Pharmaceutical Sciences*, *110*(4), 1432–1443.

Di, X., Liang, X., Shen, C., Pei, Y., Wu, B., & He, Z. (2022). Carbohydrates Used in Polymeric Systems for Drug Delivery: From Structures to Applications. *Pharmaceutics*, *14*(4), 739. https://doi.org/10.3390/pharmaceutics14040739

EMA|ICH Q2(R2). (1994). *ICH Q2(R2) Validation of analytical procedures—Scientific guideline | European Medicines Agency (EMA)*. https://www.ema.europa.eu/en/ich-q2r2-validation-analytical-procedures-scientific-guideline

Eraga, S. O., Olayemi, O. J., Obidiro, O. P., Osemeke, O. L., & Iwuagwu, M. A. (2024). Effects of starch pre-gelatinization on the physicochemical and tableting properties of a co-processed excipient for direct compression. *West African Journal of Pharmacy*, *35*(2), 118–130.

European Medicines Agency (EMA)(Ph. Eur. 2.9.34). (2013, February 11). *ICH Q4B Annex 13 Bulk density and tapped density of powders—Scientific guideline | European Medicines Agency (EMA)*. https://www.ema.europa.eu/en/ich-q4b-annex-13-bulk-density-tapped-density-powders-scientific-guideline

Ewing, A. V., Clarke, G. S., & Kazarian, S. G. (2014). Stability of indomethacin with relevance to the release from amorphous solid dispersions studied with ATR-FTIR spectroscopic imaging. *European Journal of Pharmaceutical Sciences*, *60*, 64–71.

https://www.fda.gov/industry/color-additive-inventories/color-additive-status-list. Accessed on 13th October 2019.

Fina, F., Goyanes, A., Gaisford, S., & Basit, A. W. (2017a). Selective laser sintering (SLS) 3D printing of medicines. *International Journal of Pharmaceutics*, *529*(1), 285–293. https://doi.org/10.1016/j.ijpharm.2017.06.082

Fina, F., Goyanes, A., Gaisford, S., & Basit, A. W. (2017b). Selective laser sintering (SLS) 3D printing of medicines. *International Journal of Pharmaceutics*, *529*(1–2), 285–293.

Fina, F., Goyanes, A., Gaisford, S., & Basit, A. W. (2017c). Selective laser sintering (SLS) 3D printing of medicines. *International Journal of Pharmaceutics*, *529*(1–2), 285–293.

Fina, F., Madla, C. M., Goyanes, A., Zhang, J., Gaisford, S., & Basit, A. W. (2018). Fabricating 3D printed orally disintegrating printlets using selective laser sintering. *International Journal of Pharmaceutics*, *541*(1), 101–107. https://doi.org/10.1016/j.ijpharm.2018.02.015

Garbacz, P., & Wesolowski, M. (2018). DSC, FTIR and Raman spectroscopy coupled with multivariate analysis in a study of co-crystals of pharmaceutical interest. *Molecules*, *23*(9), 2136.

Giri, B. R., Poudel, S., & Kim, D. W. (2021). Cellulose and its derivatives for application in 3D printing of pharmaceuticals. *Journal of Pharmaceutical Investigation*, *51*(1), 1–22.

Gueche, Y. A., Sanchez-Ballester, N. M., Cailleaux, S., Bataille, B., & Soulairol, I. (2021). Selective Laser Sintering (SLS), a New Chapter in the Production of Solid Oral Forms (SOFs) by 3D Printing. *Pharmaceutics*, *13*(8), 1212. https://doi.org/10.3390/pharmaceutics13081212

Hasegawa, K., Goto, S., Kataoka, H., Chatani, H., Kinoshita, T., Yokoyama, H., & Tsuchida, T. (2024). Quantification of crystallinity during indomethacin crystalline transformation from α- to γ-polymorphic forms and of the thermodynamic contribution to dissolution in aqueous buffer and solutions of solubilizer. *RSC Advances*, *14*(6), 4129–4141. https://doi.org/10.1039/D3RA08481G

Hess, S., Teubert, U., Ortwein, J., & Eger, K. (2001). Profiling indomethacin impurities using high-performance liquid chromatography and nuclear magnetic resonance. *European Journal of Pharmaceutical Sciences*, *14*(4), 301–311.

Hong, Y., Liu, G., & Gu, Z. (2016). Recent advances of starch-based excipients used in extended-release tablets: A review. *Drug Delivery*, *23*(1), 12–20. https://doi.org/10.3109/10717544.2014.913324

Hong, Y., & Liu, X. (2023). Pre-gelatinized modification of starch. In *Physical modifications of starch* (pp. 91–102). Springer.

Journal Pre-proof

Imaizumi, H., Nambu, N., & Nagai, T. (1980). Stability and several physical properties of amorphous and crystalline forms of indomethacin. *Chemical and Pharmaceutical Bulletin*, *28*(9), 2565–2569.

Kollamaram, G., Faucher, A., Croker, D. M., & Walker, G. M. (2018). Valvejet Technology for the Production of a Personalised Fixed Dose Combination of Ramipril and Glimepiride: An Investigative Study on the Stability of Ramipril. *Pharmaceutical Research*, *35*(9).

Kosaka, M., Higashi, K., Nishimura, M., Ueda, K., & Moribe, K. (2020). Clarification of the Dissolution Mechanism of an Indomethacin/Saccharin/Polyvinylpyrrolidone Ternary Solid Dispersion by NMR Spectroscopy. *Journal of Pharmaceutical Sciences*, *109*(12), 3617–3624.

Kruth, J.-P., Mercelis, P., Van Vaerenbergh, J., Froyen, L., & Rombouts, M. (2005). Binding mechanisms in selective laser sintering and selective laser melting. *Rapid Prototyping Journal*, *11*(1), 26–36.

Kruth, J.-P., Wang, X., Laoui, T., & Froyen, L. (2003). Lasers and materials in selective laser sintering. *Assembly Automation*, *23*(4), 357–371.

Kumar, S. (2003). Selective laser sintering: A qualitative and objective approach. *JOM*, *55*(10), 43–47. https://doi.org/10.1007/s11837-003-0175-y

Lam, C. X. F., Mo, X. M., Teoh, S.-H., & Hutmacher, D. W. (2002). Scaffold development using 3D printing with a starch-based polymer. *Materials Science and Engineering: C*, *20*(1–2), 49–56.

Léonard, G., Bertrand, F., Chaouki, J., & Gosselin, P. M. (2008). An experimental investigation of effusivity as an indicator of powder blend uniformity. *Particulate Processes in the Pharmaceutical Industry*, *181*(2), 149–159. https://doi.org/10.1016/j.powtec.2006.12.007

Li, J., Ahmed, H. H., Hussein, A. M., Kaur, M., Jameel, M. K., Kaur, H., Tillaeva, U., Al-Hussainy, A. F., Sameer, H. N., & Hameed, H. G. (2025). Advances in polysaccharide-based materials for biomedical and pharmaceutical applications: A comprehensive review. *Archiv Der Pharmazie*, *358*(1), e2400854.

Li, Y., Rantanen, J., Yang, M., & Bohr, A. (2019). Molecular structure and impact of amorphization strategies on intrinsic dissolution of spray dried indomethacin. *European Journal of Pharmaceutical Sciences*, *129*, 1–9.

Maddineni, S., Battu, S. K., Morott, J., Majumdar, S., Murthy, S. N., & Repka, M. A. (2015). Influence of process and formulation parameters on dissolution and stability characteristics of Kollidon® VA 64 hot-melt extrudates. *AAPS PharmSciTech*, *16*(2), 444–454.

Majumder, M., Rajabnezhad, S., Nokhodchi, A., & Maniruzzaman, M. (2018). Chemico-calorimetric analysis of amorphous granules manufactured via continuous granulation process. *Drug Delivery and Translational Research*, *8*, 1658–1669.

Maliki, S., Sharma, G., Kumar, A., Moral-Zamorano, M., Moradi, O., Baselga, J., Stadler, F. J., & García-Peñas, A. (2022). Chitosan as a Tool for Sustainable Development: A Mini Review. *Polymers*, *14*(7), 1475. https://doi.org/10.3390/polym14071475

Maniruzzaman, M., Ross, S. A., Dey, T., Nair, A., Snowden, M. J., & Douroumis, D. (2017). A quality by design (QbD) twin—Screw extrusion wet granulation approach for processing water insoluble drugs. *International Journal of Pharmaceutics*, *526*(1), 496–505. https://doi.org/10.1016/j.ijpharm.2017.05.020

Michailova, V., Titeva, S., Kotsilkova, R., Krusteva, E., & Minkov, E. (2001). Influence of hydrogel structure on the processes of water penetration and drug release from mixed hydroxypropylmethyl cellulose/thermally pregelatinized waxy maize starch hydrophilic matrices. *International Journal of Pharmaceutics*, *222*(1), 7–17.

Mohamed EM, Barakh Ali SF, Rahman Z, Dharani S, Ozkan T, Kuttolamadom MA, Khan MA. Formulation Optimization of Selective Laser Sintering 3D-Printed Tablets of Clindamycin Palmitate Hydrochloride by Response Surface Methodology. AAPS PharmSciTech. 2020 Aug 13;21(6):232. Doi: 10.1208/s12249-020-01775-0. PMID: 32794080.

Mohapatra, S., Samanta, S., Kothari, K., Mistry, P., & Suryanarayanan, R. (2017). Effect of polymer molecular weight on the crystallization behavior of indomethacin amorphous solid dispersions. *Crystal Growth & Design*, *17*(6), 3142–3150.

Murkute, M. P. S., Gaikwad, M. R. G., Kathar, M. N. P., Sanap, D. G. S., & Raut, M. R. S. (2022). 3D PRINTING TECHNOLOGY AND SHORT INTRODUCTION IN 3D BIO-PRINTED MATRICES FOR IN VITRO TUMOR MODEL. *International Journal of Scientific Development and Research*, *7*(2), 217–228. https://doi.org/10.1729/Journal.29443

Musumeci, D., Zhou, J., Xie He, J., Rades, T., & Martins, I. C. (2025). Is There Polyamorphism in Amorphous Indomethacin? Investigating the Physicochemical Properties of Amorphous Indomethacin with Different Thermal History. *Molecular Pharmaceutics*, *22*(4), 2065–2076.

Narala, S., Nyavanandi, D., Mandati, P., Youssef, A. A. A., Alzahrani, A., Kolimi, P., Zhang, F., & Repka, M. (2023). Preparation and in vitro evaluation of hot-melt extruded pectin-based pellets containing ketoprofen for colon targeting. *International Journal of Pharmaceutics: X*, *5*, 100156. https://doi.org/10.1016/j.ijpx.2022.100156

Norman, J., Madurawe, R. D., Moore, C. M., Khan, M. A., & Khairuzzaman, A. (2017). A new chapter in pharmaceutical manufacturing: 3D-printed drug products. *Advanced Drug Delivery Reviews*, *108*, 39–50.

Nováková, L., Matysová, L., Havlíková, L., & Solich, P. (2005). Development and validation of HPLC method for determination of indomethacin and its two degradation products in topical gel. *Journal of Pharmaceutical and Biomedical Analysis, Selected Papers from the 15th International Symposium on Pharmaceutical and Biomedical Analysis*, *37*(5), 899–905. https://doi.org/10.1016/j.jpba.2004.09.012

Journal Pre-proof

Nyavanandi, D., Kallakunta, V. R., Sarabu, S., Butreddy, A., Narala, S., Bandari, S., & Repka, M. A. (2021). Impact of hydrophilic binders on stability of lipid-based sustained release matrices of quetiapine fumarate by the continuous twin screw melt granulation technique. *Advanced Powder Technology*, *32*(7), 2591–2604.

PA Cuthbert & Co. (2023, November 6). *Enhance Tablet Quality With Starch 1500—Pacco Tablet Solutions*. https://pacuthbert.co.za/core-excipients-starch-1500/

Petruševska, M., Berglez, S., Krisch, I., Legen, I., Megušar, K., Peternel, L., Abrahamsson, B., Cristofoletti, R., Groot, D. W., & Kopp, S. (2015). Biowaiver monographs for immediate release solid oral dosage forms: Levetiracetam. *Journal of Pharmaceutical Sciences*, *104*(9), 2676–2687.

Pham, T. N., Watson, S. A., Edwards, A. J., Chavda, M., Clawson, J. S., Strohmeier, M., & Vogt, F. G. (2010). Analysis of Amorphous Solid Dispersions Using 2D Solid-State NMR and 1H T1 Relaxation Measurements. *Molecular Pharmaceutics*, *7*(5), 1667–1691. https://doi.org/10.1021/mp100205g

Pillai A. (2023). *Pillai, A., Chakka, J., Heshmathi, N., Zhang, Y., Alkadi, F., & Maniruzzaman, M. (2023). Multifunctional three-dimensional printed copper loaded calcium phosphate scaffolds for bone regeneration. Pharmaceuticals, 16(3), 352.*

Pratik, J., Rupesh, T., & Raosaheb, S. (2019). A brief review on Kollidon. *Journal of Drug Delivery & Therapeutics*, *9*(2), 493–500.

Sabbatini, B., Cambriani, A., Cespi, M., Palmieri, G. F., Perinelli, D. R., & Bonacucina, G. (2021). An Overview of Natural Polymers as Reinforcing Agents for 3D Printing. *ChemEngineering*, *5*(4), 78. https://doi.org/10.3390/chemengineering5040078

Sheng, X. (2009a). *Drug dissolution from pregelatinized corn starch capsules*. Purdue University.

Sheng, X. (2009b). *Drug dissolution from pregelatinized corn starch capsules—ProQuest, 2009*. https://www.proquest.com/docview/304989493?%20Theses&fromopenview=true&pq-origsite=gscholar&sourcetype=Dissertations%20

Shimada, Y., Komaki, H., Hirai, A., Goto, S., Hashimoto, Y., Uchiro, H., & Terada, H. (2018). Decarboxylation of indomethacin induced by heat treatment. *International Journal of Pharmaceutics*, *545*(1–2), 51–56.

Simpson, D. B. B. (2000). *Starch 1500*. University of Bath (United Kingdom).

Sridhar, V. (2013). *Solubility improvement by solid dispersion and their characterization: Indomethacin and phenytoin*. University of Toledo.

Strojewski, D., & Krupa, A. (2022). Kollidon® VA 64 and Soluplus® as modern polymeric carriers for amorphous solid dispersions. *Polymers in Medicine*, *52*(1), 19–29.

Journal Pre-proof

Su, L., Feng, Y., Wei, K., Xu, X., Liu, R., & Chen, G. (2021). Carbohydrate-Based Macromolecular Biomaterials. *Chemical Reviews*, *121*(18), 10950–11029. https://doi.org/10.1021/acs.chemrev.0c01338

Suwanprateeb, J., Sanngam, R., & Panyathanmaporn, T. (2010). Influence of raw powder preparation routes on properties of hydroxyapatite fabricated by 3D printing technique. *Materials Science and Engineering: C*, *30*(4), 610–617.

Szafraniec-Szczęsny, J., Antosik-Rogóż, A., Kurek, M., Gawlak, K., Górska, A., Peralta, S., Knapik-Kowalczuk, J., Kramarczyk, D., Paluch, M., & Jachowicz, R. (2021). How Does the Addition of Kollidon®VA64 Inhibit the Recrystallization and Improve Ezetimibe Dissolution from Amorphous Solid Dispersions? *Pharmaceutics*, *13*(2), 147. https://doi.org/10.3390/pharmaceutics13020147

Tabriz, A. G., Kuofie, H., Scoble, J., Boulton, S., & Douroumis, D. (2023). Selective Laser Sintering for printing pharmaceutical dosage forms. *Journal of Drug Delivery Science and Technology*, *86*, 104699. https://doi.org/10.1016/j.jddst.2023.104699

Tabriz, A., Junqueira, L. A., Kolipaka, S. S., Hui, H.-W., Boersen, N., Roberts, S., Jones, J., & Douroumis, D. (2025). Printabily of Pharmaceutical-Grade Polymers using Selective Laser Sintering with a CO2 Laser. *AAPS PharmSciTech*, *26*(5), 144. https://doi.org/10.1208/s12249-025-03141-4

Taylor, L. S., & Zografi, G. (1997a). Spectroscopic characterization of interactions between PVP and indomethacin in amorphous molecular dispersions. *Pharmaceutical Research*, *14*, 1691–1698.

Taylor, L. S., & Zografi, G. (1997b). Spectroscopic Characterization of Interactions Between PVP and Indomethacin in Amorphous Molecular Dispersions. *Pharmaceutical Research*, *14*(12), 1691–1698. https://doi.org/10.1023/A:1012167410376

Thakkar, R., Jara, M. O., Swinnea, S., Pillai, A. R., & Maniruzzaman, M. (2021). Impact of Laser Speed and Drug Particle Size on Selective Laser Sintering 3D Printing of Amorphous Solid Dispersions. *Pharmaceutics*, *13*(8), Article 8. https://doi.org/10.3390/pharmaceutics13081149

Thakkar, R., Zhang, Y., Zhang, J., & Maniruzzaman, M. (2021). Synergistic application of twin-screw granulation and selective laser sintering 3D printing for the development of pharmaceutical dosage forms with enhanced dissolution rates and physical properties. *European Journal of Pharmaceutics and Biopharmaceutics*, *163*, 141–156. https://doi.org/10.1016/j.ejpb.2021.03.016

Thiptinnakorn, T., Wangnonglad, P., & Wasombat, R. (2020). Effect of pregelatinized starch on dissolution of paracetamol extended release bilayer tablets. *วารสาร วิทยาศาสตร์และ เทคโนโลยี หัวเฉียว เฉลิมพระเกียรติ*, *6*(1), 7–17.

Trenfield, S. J., Awad, A., Goyanes, A., Gaisford, S., & Basit, A. W. (2018). 3D Printing Pharmaceuticals: Drug Development to Frontline Care. *Trends in Pharmacological Sciences*, *39*(5), 440–451. https://doi.org/10.1016/j.tips.2018.02.006

Tres, F., Treacher, K., Booth, J., Hughes, L. P., Wren, S. A., Aylott, J. W., & Burley, J. C. (2016). Indomethacin-Kollidon VA64 extrudates: A mechanistic study of pH-dependent controlled release. *Molecular Pharmaceutics*, *13*(3), 1166–1175.

USP (616). (2015). *〈616〉 Bulk Density of Powders*. https://doi.org/10.31003/USPNF_M99375_03_01

USP〈1174〉. (2024). *〈1174〉 Powder Flow https://online.uspnf.com/uspnf/document/1_GUID-D48AA926-0912-4F7D-8B2B-3A022A1196FE_2/ 01-May-2024*. https://doi.org/10.31003/USPNF_M99885_02_01

USPNF Monograph. (2025). *Indomethacin Extended-Release Capsules/ Current DocID: GUID-11C71173-FC5C-4E9C-A4D4-6E8D68C97D62_5_en-US/USP43-NF38/https://doi.org/10.31003/USPNF_M40421_05_01/ 01 Aug 2025*.

Viidik, L., Vesala, J., Laitinen, R., Korhonen, O., Ketolainen, J., Aruväli, J., Kirsimäe, K., Kogermann, K., Heinämäki, J., & Laidmäe, I. (2021). Preparation and characterization of hot-melt extruded polycaprolactone-based filaments intended for 3D-printing of tablets. *European Journal of Pharmaceutical Sciences*, *158*, 105619.

Wei, Q., Zhou, J., An, Y., Li, M., Zhang, J., & Yang, S. (2023). Modification, 3D printing process and application of sodium alginate based hydrogels in soft tissue engineering: A review. *International Journal of Biological Macromolecules*, *232*, 123450. https://doi.org/10.1016/j.ijbiomac.2023.123450

Wu, B. M., Borland, S. W., Giordano, R. A., Cima, L. G., Sachs, E. M., & Cima, M. J. (1996). Solid free-form fabrication of drug delivery devices. *Journal of Controlled Release*, *40*(1), 77–87. https://doi.org/10.1016/0168-3659(95)00173-5

Xi, Z., Zhang, W., Fei, Y., Cui, M., Xie, L., Chen, L., & Xu, L. (2020a). Evaluation of the solid dispersion system engineered from mesoporous silica and polymers for the poorly water soluble drug indomethacin: In vitro and in vivo. *Pharmaceutics*, *12*(2), 144.

Xi, Z., Zhang, W., Fei, Y., Cui, M., Xie, L., Chen, L., & Xu, L. (2020b). Evaluation of the Solid Dispersion System Engineered from Mesoporous Silica and Polymers for the Poorly Water Soluble Drug Indomethacin: In Vitro and In Vivo. *Pharmaceutics*, *12*(2), 144. https://doi.org/10.3390/pharmaceutics12020144

Xu, P., Li, J., Meda, A., Osei-Yeboah, F., Peterson, M. L., Repka, M., & Zhan, X. (2020). Development of a quantitative method to evaluate the printability of filaments for fused deposition modeling 3D printing. *International Journal of Pharmaceutics*, *588*, 119760.

Journal Pre-proof

Yang, Y., Xu, Y., Wei, S., & Shan, W. (2021). Oral preparations with tunable dissolution behavior based on selective laser sintering technique. *International Journal of Pharmaceutics*, *593*, 120127. https://doi.org/10.1016/j.ijpharm.2020.120127

Zamboulis, A., Michailidou, G., Koumentakou, I., & Bikiaris, D. N. (2022). Polysaccharide 3D Printing for Drug Delivery Applications. *Pharmaceutics*, *14*(1), 145. https://doi.org/10.3390/pharmaceutics14010145

Zarandona, I., Bengoechea, C., Álvarez-Castillo, E., de la Caba, K., Guerrero, A., & Guerrero, P. (2021). 3D Printed Chitosan-Pectin Hydrogels: From Rheological Characterization to Scaffold Development and Assessment. *Gels*, *7*(4), 175. https://doi.org/10.3390/gels7040175

Zhang, Y., Thakkar, R., Zhang, J., Lu, A., Duggal, I., Pillai, A., Wang, J., Aghda, N. H., & Maniruzzaman, M. (2023). Investigating the Use of Magnetic Nanoparticles As Alternative Sintering Agents in Selective Laser Sintering (SLS) 3D Printing of Oral Tablets. *ACS Biomaterials Science & Engineering*, *9*(6), 2924–2936. https://doi.org/10.1021/acsbiomaterials.2c00299

Declaration of interests

☐ The authors declare that they have no known competing financial interests or personal relationships that could have appeared to influence the work reported in this paper.

☒The authors declare the following financial interests/personal relationships which may be considered as potential competing interests:

The authors declare the following financial interests/personal relationships which may be considered as potential competing interests: Mohammed Maniruzzaman (M.M.), an author of this manuscript, holds stock in, serves on a scientific advisory board for, or is a consultant for CoM3D Ltd. (Surrey, UK), DosePlus Therapeutics, Inc. (Princeton, NJ, USA), SmarGic Tech LLC (Oxford, MS, USA), and Septum Solutions LLC (Houston, TX, USA). Yu Zhang (Y.Z.) also holds stocks in SmarGic Tech LLC (Oxford, MS, USA). The companies had no role in the design of the study; in the collection, analyses, or interpretation of data; in the writing of the manuscript; and in the decision to publish the results. If there are other authors, they declare that they have no known competing financial interests or personal relationships that could have appeared to influence the work reported in this paper.

Journal Pre-proof